2017

QUANTIFYING CURRENT SEDIMENT DEPOSITION, LEGACY SEDIMENTS, AND PRE-IMPOUNDMENT VERTICAL ACCRETION AND CARBON DYNAMICS FOLLOWING DAM REMOVAL IN A RECENTLY RESTORED TIDAL FRESHWATER WETLAND

Melissa J. Davis
Virginia Commonwealth University

Quantifying current sediment deposition, legacy sediments, and pre-impoundment vertical accretion and carbon dynamics following dam removal in a recently restored tidal freshwater wetland

A thesis submitted in partial fulfillment of the requirements for the degree of Master of Science in Environmental Studies at Virginia Commonwealth University.

by

Melissa Joanne Davis

M.S. ENVS, Virginia Commonwealth University, 2017

B.A., ENVS, Virginia Commonwealth University, 2013

Director: Dr. Edward Crawford

Deputy Director of the VCU Rice Rivers Center, Center for Environmental Studies

Virginia Commonwealth University

Richmond, Virginia

August, 2017

Acknowledgment

The author wishes to thank several people. I would like to thank my family and Scott Schibner for their generous love, patience and support during my Masters work. I would like to express my sincere gratitude to Dr. Edward Crawford for fostering my education in wetland and restoration ecology along with six years of amazing academic and professional mentorship. I would like to thank Dr. Arif Sikder for his support and guidance in collecting and interpreting sediment core data as well as sitting in on my committee. I would also like to thank Dr. Stephen McIninch for being a part of my committee and for his continued assistance as M.S. program director for the Center for Environmental Studies. I wish to thank Jennifer Ciminelli for sitting in on my committee, fostering my geospatial education and for her emotional support and guidance throughout my Masters work. Thank you to Ron Lopez for his tireless efforts in fieldwork, brainstorming sessions and continual support throughout this research project. I would like to acknowledge all of the undergraduate volunteers, in particular, Chris Gatens and Sara Sanderlin, for their assistance in vigorous fieldwork and data collection. I would like to thank Xin-Chen Liu for his assistance in running XRF analysis and his help in the field. Furthermore, I would like to also acknowledge the University of Georgia Isotope Lab for conducting our radiocarbon dating as well as Dr. Paul Bukaveckas and the EAL lab for assistance and use of their lab for C: N ratio analyses. Lastly, I would like to extend a special thank you to the VCU Rice Rivers Center research grant program that made much of this research feasible.

Table of Contents

List of Tables

List of Figures

Abstract

QUANTIFYING CURRENT SEDIMENT DEPOSITION, LEGACY SEDIMENTS, AND PRE-IMPOUNDMENT VERTICAL ACCRETION AND CARBON DYNAMICS FOLLOWING DAM REMOVAL IN A RECENTLY RESTORED TIDAL FRESHWATER WETLAND

By Melissa Joanne Davis, M.S. ENVS

A thesis submitted in partial fulfillment of the requirements for the degree of Master of Science in Environmental Studies at Virginia Commonwealth University.

Virginia Commonwealth University, 2017.

Major Director: Dr. Edward Crawford, Deputy Director of the VCU Rice Rivers Center, Center for Environmental Studies

Damming disrupts natural sediment flow to downstream resulting in legacy sediment accumulation. Legacy sediments have been well investigated in streams throughout the Piedmont region; however, there is no research of legacy sediments following dam removal in low-gradient Coastal Plain streams. Research objectives were to: characterize legacy sediments in a low-gradient stream restoration, quantify pre-impoundment accretion and carbon dynamics, and assess current sediment deposition rates via ^{14}C analyses within sediment cores and sediment collection tiles. Carbon accumulation and accretion rates of modern tidal sediment have reached that of the tidal relic benchmark and current sediment deposition rates are similar between the natural reference and restored tidal wetlands. At this site, the pattern of legacy sediment accumulation and stream incision was reversed relative to previous studies in higher gradient systems. Results suggest in dam impacted Coastal Plain streams, legacy sediment may become a benefit rather than a liability for downstream tidal wetlands.

Introduction

Wetlands provide a multitude of ecosystem services and functions including filtration of incoming ocean, river water and terrestrial runoff making them critical for maintaining healthy coastal and ocean ecosystems (Mitsch and Gosslink, 2007). Wetlands also play a disproportionately large role in global carbon cycling due to slowed rates of decomposition in water-saturated anaerobic soils coupled with high rates of primary productivity (Morrissey et al., 2014). While only comprising 5-8% of the terrestrial land surface area (Mitsch and Gosslink, 2007) wetlands are estimated to store 45-70% of all terrestrial carbon (Mitra et al., 2005). Moreover, tidal wetlands provide vital nursery habitat for anadromous and other migratory fishes, as such, reestablishing tidal communication through dam removal in tidal wetlands is an important step for maintaining sustainable fishery stocks (Bednarek, 2001). Wetlands also stabilize shorelines through aggregation of soils by wetland vegetation and provide critical floodwater storage making coastal communities that conserve and restore wetlands more resilient and sustainable (Gedan et al., 2011).

Tidal freshwater wetlands (TFWs), situated at the head of estuaries, are some of the first ecosystems to receive and remove watershed-derived sediment and nutrient pollution (Neubauer et al., 2002). TFWs ability to filter nutrients and sediment is highly valued as excessive sediment and nutrient loading as a result of anthropogenic activity is widespread in the Chesapeake Bay watershed and throughout the U.S. (Kemp et al., 2005). While these ecosystems are some of the most valuable in the world for their filtration ability and wildlife habitat (Cooper et al. 2008;

Craft et al. 2009) they are also considered some of the most vulnerable. In the face of global climate change, these ecosystems are threatened by increasing rates of relative sea level rise (RSLR) coupled with decreased inputs of fluvial sediments (Kirwan and Megonigal 2013; Weston, 2014; Palinkas and Engelhardt, 2016).

Rising sea levels may lead to freshwater ecosystems experiencing widespread saltwater intrusion, which has been shown to alter primary production (Baldwin and Mendelssohn, 1998), microbial metabolism (Weston et al., 2011; Neubauer et al., 2013), and nutrient cycling (Morrissey et al., 2014). TFWs are of particular concern as they are critical in biogeochemical cycling because of the hydrologic connectivity with adjoining rivers (Ensign et al., 2013). Studies have shown salt-water intrusion could increase microbial decomposition rates in these freshwater ecosystems which may lead to decreased carbon sequestration, vertical accretion, and soil organic matter (O.M.) accumulation (Morrissey et al., 2014).

Steady soil accretion, (net balance between sediment deposition and removal processes such as microbial utilization of organic carbon) increases surface elevation in tidal wetlands (Neubauer et al., 2002, Butzeck et al., 2014). This allows vegetation to persist as long as the rate of accretion exceeds that of RSLR. However, if RSLR outpaces accretion, tidal wetlands will be lost along with their associated ecosystem services. Currently, there is a lack of research on TFWs' ability to keep pace with RSLR as most sedimentation studies have focused on salt marshes (e.g. Morris et al., 2002; Reed, 2002; Nielsen and Nielsen, 2002; Neumeier and Amos, 2006; Van Proosdij et al., 2006; D'Alpaos et al., 2007) few have been conducted in TFWs (e.g., Khan and Brush 1994; Pasternack and Brush, 2001; Neubauer et al., 2002; Neubauer, 2008). The cumulative findings of TFW accretion suggest current rates of sediment accretion may not be able to maintain positive surface elevation relative to sea level rise. However, sediment accretion in TFWs is highly variably both spatially and temporally (Barendregt and Swarth, 2013).

While these threats pertain to natural TFWs, restored TFWs may be at even greater risk and represent an even larger gap in the current literature. Staggering rates of wetland loss and the following recognition of wetland values and functions have stimulated restoration efforts worldwide. With policies in place such as "No Net Loss" of wetlands here in the U.S., efforts of conservation and restoration have become an increasingly popular industry (Mitsch and Gosselink, 2007). Quantifying restoration success is often elusive, and typically lacks acknowledgement of differences in biogeochemical functioning between natural and restored wetlands as most measures of success are based on vegetation criteria. It has been observed that prior land use of restored wetlands can alter rates of soil O.M. accumulation in turn limiting microbial metabolism and vertical accretion (Crawford et al., 2005; Crawford, 2002). Therefore, restored TFWs may be more vulnerable to sea level rise due to the combined impacts from flooding, salt-water intrusion and inherent factors associated with prior land use.

Current research of freshwater wetland soils has assessed and reported smaller stocks of soil organic carbon in restored and created wetlands compared to natural reference wetlands (Crawford et al., 2007). A majority of these studies focus on sites restored from agricultural draining of non-tidal depressional wetlands (e.g. Fennessy et al., 2008, Ballatine and Schneider 2009, Marton et al., 2014). Carbon sequestration and accretion dynamics in TFWs restored following dam removal is poorly understood. The U.S. Army Corps of Engineers estimates there are over 80,000 dams greater than 6 feet and tens of thousands of smaller dams across the U.S., of which the majority are unsafe, old, or no longer serve their intended purpose. In Virginia, of the 2,919 established dams, over a third (1,019) are labeled as either high or significant for hazard potential (USACE National Inventory of Dams, 2017). The removal of dams and the subsequent restoration of wetlands and streams are going to continue to grow in importance, increasing the need for comprehensive restoration research to help guide future restoration efforts.

Damming disrupts the natural flow of sediment to adjoining water bodies which results in the accumulation of what is commonly referred to as Legacy Sediments (LS). Extensive research surrounding LS has been conducted in the Mid-Atlantic Piedmont region were milldam establishment has been widespread and pervasive throughout the early 19th century (Merritts et al., 2011). A majority of the current literature has been focused on the geomorphological impact of dams and the subsequent effects of LS post dam removal. The establishment of dams has been tied to a rise in stream base level and reduction in valley slope as a result of reservoir sedimentation. Subsequently, a drop in base level and an increase in slope, suspended sediment loads, bank erosion and stream incision have all been observed post dam removal (Walter and Merritts, 2008; Merritts et al., 2011; Donovan et al., 2015; Lyons et al., 2015).

While impacts of dam establishment and the following deposition of LS has been well investigated in lotic Mid-Atlantic Piedmont region (e.g., Walter and Merritts, 2008; Merritts et al., 2011; Hupp et al., 2013; Donovan et al., 2015; Lyons et al., 2015) there has been little research of LS following dam removal in low-gradient Coastal Plain streams. In this study we have the unique opportunity to elucidate the impacts of impoundment and LS in a low-gradient, tidal and non-tidal Coastal Plain stream and its surrounding wetlands. To fully investigate the impacts of damming it is vital to not only address the current variations in sediment deposition but also establish a baseline of accretion and carbon dynamics during impoundment and prior to the landscape modifications that have disturbed the dynamic equilibrium of this stream and its wetlands. Therefore, the objectives of this study were to:

1. Quantify spatial and temporal variations of LS characteristics in a low-gradient tidal stream restoration within the lower James River watershed.
2. Establish the historical reference of carbon sequestration and accretion rates of the pre-impoundment forested freshwater wetland environment to create a benchmark for the restoration efforts as well as isolate the impacts of impoundment on wetland function and accretion.
3. Assess the current temporal and spatial variability in sediment deposition within the recently restored Kimages Creek wetlands and adjacent, unaltered wetlands of Harris Creek to investigate current sedimentation processes in a restoration setting.

Methods

Site Description

This study took place at the Virginia Commonwealth University Rice Rivers Center (RRC), located on the lower James River in Charles City County, Virginia (Figure 1). Kimages Creek (KC), a second order Coastal Plain stream, was dammed in 1927 at its confluence with the James River creating a 72-acre impoundment known as Lake Charles. Prior to damming, the KC basin included both tidal and non-tidal forested freshwater wetlands, which were logged in 1862 and prior to dam establishment in 1927. The dam was partially breached due to a period of heavy rainfall in 2006. By spring 2008, tidal communication was restored when the breach incised to a depth below high tide level of the James River Estuary (Bukaveckas and Wood, 2014). Partial removal of the dam was then carried out in December 2010 (Jones, 2011). A timeline from impoundment phase to partial dam removal is depicted in Figure 2.

After tidal connection was reestablished efforts have been ongoing to restore the wetlands back to their original forested state. Currently, the wetlands are primarily freshwater tidal and non-tidal marshes; dominant species include *Typha angustifolia* (cattail), *Murdannia keisak* (asian spiderwort), *Polygonum sagittatum* (arrowleaf tearthumb), *Leersia oryzoides* (rice cutgrass), *Juncus effusus* (softrush), *Pontedaria cordata* (pickerelweed), and *Saggitaria latifolia* (broadleaf arrowhead). Natural woody recruitment includes *Acer rubrum* (red maple), *Liquidambar styraciflua* (sweet gum), *Salix nigra* (black willow), and *Platanus occidentalis* (sycamore) (Bukaveckas and Wood, 2014). The KC watershed is mostly comprised of forest

(70%) and other natural areas (11% old fields and wetlands 12%) with a small percentage under cultivation (7%) (Bukaveckas and Wood, 2014).

The RRC also contains Harris Creek (HC), a relatively undisturbed neighboring creek that is serving as a benchmark and reference site for the KC restoration. The tidal freshwater-forested wetlands of HC are dominated by woody species including *Taxodium distichum* (bald cypress), *Fraxinus* spp. (ash), *Nyssa biflora* (swamp tupelo), and *Acer rubrum* along with an understory comprised primarily of herbaceous species such as *Peltandra virginica* (arrow arum), *Murdannia keisak*, *Polygonum sagittatum* (arrowleaf tearthumb), and *Pontedaria cordata* (Deemy, 2012).

Contemporary variation in sediment deposition

Beginning July 2015 through June 2016, net sediment deposition was measured using sediment collection tiles (SCTs) within HC and KC wetlands following the protocol of Pasternack and Brush, (1998) and Christiansen et al., (2000). The SCTs were 117 cm^2 ceramic, glazed tiles with an anchored PVC design modified after Pasternack and Bursh, (1998); a basic schematic is depicted in Figure 3. A total of 8 transects were established spanning elevational gradients from creekbank to toe of slope. Individual transects were located along a north to south latitudinal gradient within each creek. There were 3 transects (n=27 SCTs) within Harris Creek, 3 transects (n=27 SCTs) within the tidal portion of Kimages Creek, and 2 transects (n=12 SCTs) within the non-tidal portion of Kimages Creek. In the tidal transects tiles were arranged in a block design with each block containing 3 SCTs (block A was situated closest to creek bank, block B was representing interior wetland and block C was closest to toe of slope, Figure 4).

SCTs were deployed and sampled during low tides and the deposited sediments were collected from each tile every other week during the growing season (April-August) and once a month thereafter. Simultaneously, surface core samples were collected (0-1 cm depth) within 1 meter of the tiles to calculate bulk density. Both tile and surface core samples were dried at 50°C for 72 hours and weighed to calculate sediment deposition rates (SDRs) and bulk density, respectively. Tile subsamples were combusted at 450°C for 12 hours and reweighed to calculate organic matter content based on weight loss-on-ignition.

Inundation (distance from primary sediment source i.e. stream) and vegetation parameters (aboveground biomass and vegetation structure) were measured as predictor variables to examine their potential influence on SDRs. Distance from sediment source to each SCT location was determined using the georeferenced GPS points of the SCTs measured to the creek center using the analysis tools on ArcMap GIS software. Aboveground biomass was assessed via vegetation surveys conducted in 1 m^2 plots selected at random within each of the 3 locations per transect using a quadrat. Sampling occurred at peak growing season in 2015 and winter of 2016, and included stem counts and species identification.

Stream morphometry of Kimages Creek was analyzed to establish an understanding of stream bank stability and floodplain connectivity as it relates to current rates of sediment deposition. Morphometrics data (slope, sinuosity, and width-to-depth ratios) was collected in 2016 while surveying the elevational gradients in the stream and surrounding floodplain in 19 stream cross-sections located throughout the KC basin. This data was gathered as part of the on-going stream restoration monitoring program and a map of the 19 cross-sections is depicted in Figure 5.

Historic variation in sediment accretion and legacy sediment characterization

Using the standard penetration test coupled with current stratigraphic information of the site, a series of 5', 10', and 15', 2" diameter PVC pipes were hand driven using a pole driver into the KC tidal and non-tidal wetlands. The cores were extracted in May of 2016 using pipe wrenches after refusal during hand driving was met. The tidal core was taken from a location were the current tidal forces are minimal as to maximize chance of capturing potential legacy sediments and limit chance of LS being eroded post dam removal. The non-tidal core was taken in the northern-most and central portion of the non-tidal wetland and a map of the core locations is shown in Figure 4. Georefernce GPS points were taken using Trimble GeoX 7,000 series handheld unit at both core locations. Vertical elevation (NAVD 88) of the sediment surface was surveyed using a Trimble R9 Kinematic Base Station located over a benchmark within the site.

A circular saw was used to cut the PVC pipes in half length-wise without cutting into the sediment as to not disturb or contaminate the samples. The sediment within the cores was then slit in half using thin metal wire. The tidal core, when all segments were combined (5', 10', and 15' PVCs), was 3.2 m in length while the non-tidal combined core was approximately 2.1 m. The cores were segmented into 10 cm intervals and samples were taken for analysis of organic content and bulk density as explained in SCTs methods above. Cores were described for visible organic detritus, texture, and colour using the Munsell soil color chart. Interval samples were also analyzed for percents carbon and nitrogen using a Fison model EA 1108 elemental analyzer after being homogenized using a mortar and pestle. The elemental composition of samples throughout cores was determined through XRF (X-ray fluorescence) analysis that was further used to calculate the chemical index of alteration (CIA), a commonly used chemical weathering index for sediments (Harnois, 1988; Nesbitt and Young, 1982; Price and Velbel, 2003) using Equation 1 below:

$$CIA = \frac{\mathrm{Al2O3}}{(\mathrm{Al2O3 + Na2O + CaO + K2O})} * 100$$

A total of five samples, three from the tidal core and two from the non-tidal core, were sent to the Center for Applied Isotope Studies at the University of Georgia for ^{14}C dating. The three samples submitted for ^{14}C dating in the tidal core were located at 0.7 m, 1.4 m, and 3.0 m below sediment surface and samples from the non-tidal core were located 1.2 m, and 2.0 m below surface. Intervals between aged samples were grouped for statistical analysis and comparisons of vertical and carbon accretion rates. Vertical accretion rates (mm y^{-1}) were converted into carbon accretion rates by combining carbon content and bulk densities shown in Equation 2 below, following Neubauer et al., 2002:

$$CA = \frac{\sum_{i=1}^{n}(\mathrm{di\ x\ Bi\ x\ Ci})}{t}$$

where CA is carbon accretion (g C m^{-2} y^{-1}); n is the number of intervals between aged markers; d_i is the thickness of the interval *i* (m); B_i is the interval bulk density (g sediment m^{-3}); and C_i is percent carbon of the interval; t is the number of years between aged markers.

<u>Statistical analyses</u>

All data were statistically analyzed using JMP statistical software. one-way Analysis of variances (ANOVAs) were used to compare SDRs, bulk density, %O.M., and stem density counts across sites and between transects within sites. Tukey HSD multiple comparison tests were used in conjunction with ANOVAs and two-sample *t*-tests were used to compare data between HC and KC tidal. Simple linear regressions were run to estimate influence of stem density, distance to sediment source, and monthly precipitation on SDRs. Paired *t*-tests were used to compare %O.M., bulk density, %C, %N, C: N molar ratios, and CIA between segments within a core. A series of two-sample *t*-tests were used to compare that same data between segments of two different cores. Brown-Forsythe tests were used when checking for equal variances and Q-Q plots were used to address the assumption of normality. In cases in which normality was not met, the Wilcoxon signed Rank test and the non-parametric Wilcoxon test were used for paired *t*-test and two-sample *t*-test, respectively.

Results

Contemporary variation in sediment deposition

Measures of sediment deposition from SCTs revealed considerable spatial variability both along the tidal to non-tidal gradient (across transects) as well as along the elevational gradient from creek banks to upland edge (within transects). Within transects, variability of sediment deposition was very high as coefficients of variation ranged between 114 to 132%, 87 to 144%, and 148 to 224% across Harris Creek, Kimages Creek tidal and Kimages Creek non-tidal, respectively. Spatial variation across transect locations (HC, KC tidal and KC non-tidal) were also high but considerably lower than that found within transects (coefficients of variations for HC, KC tidal, and KC non-tidal being: 98.68%, 77.62%, and 92.68%, respectively).

There were no significant differences in SDRs found along the north to south latitudinal gradient (across transects) within the HC or KC tidal sites. However, statistically significant differences within the elevational gradient (across blocks) were observed at both HC and KC tidal sites. Within HC, blocks A, had significantly higher SDRs than both blocks B and C (ANOVA, F=16.53, DF=2, P<0.0001, Figure 6). The same trends were found in KC tidal (ANOVA, F= 15.22, DF=2, P<0.0001, Figure 7). No significant differences in SDRs were found between the two KC non-tidal transects. SDRs were not significantly different between HC and KC tidal however; both HC and KC tidal had significantly higher SDRs than KC non-tidal (ANOVA, F= 8.96, DF=2, P<0.0002, Figure 8).

To further assess variations along the elevational gradient simple linear regressions were used to estimate the relationship between sediment deposition and distance from sediment source (i.e. stream centerline). Significant regression equations were found for each site, however small coefficients of determination revealed distance to sediment source had low predictive power on SDRs (HC: $P<0.0001$, $r^2=0.1811$; KC tidal: $P<0.0001$, $r^2=0.1381$; KC non-tidal: $P<0.0001$, $r^2=0.3884$, Figures 9-11, respectively).

Temporal variations

Over the sampling period, SDRs showed considerable temporal variation with greatest rates of sedimentation occurring during the growing season across all transects. Average transect SDRs in the growing season for HC, KC tidal, and KC non-tidal were all significantly higher than winter rates (*t*-test, $P= 0.0024$; *t*-test, $P=0.0067$; *t*-test, $P=0.0269$ for HC, KC Tidal and KC NT, respectively, Table 1). In particular, highest SDRs across all transects occurred in May 2016 which also had the highest precipitation recorded for the sampling period (Figures 12 and 13). Simple linear regressions were run to assess the influence of average monthly precipitation on SDRs. Significant regression equations were found across all sites along with high r^2 values, particularly in the tidal sites, indicating precipitation had high predictive power on SDRs over the sampling period (HC: $P<0.0001$, $r^2=0.5469$; KC tidal: $P<0.0001$, $r^2=0.6545$; KC non-tidal: $P=0.0301$, $r^2=0.1964$, Figures 14-16, respectively).

Above ground biomass density

Stem density in the KC non-tidal transects were dominated by grass species, primarily *Leersia oryzoides* while stem counts in HC were dominated by *Murdannia keisak*, *Peltandra virginica* and *Polygonum sagittatum.* Stem counts in the tidal transects of KC were dominated by either *Murdannia keisak* or a combination of *Murdannia keisak* and *Typha latifolia*. Generally, higher stem counts were observed in the growing season for the tidal transects however, no significant differences in stem density were found between seasons. Total stem counts, (growing season and winter), in HC and KC tidal were not significantly different from each other but both had significantly lower stem counts than KC non-tidal (ANOVA, F= 7.55, DF=2, P<0.0018, Table 2). Simple linear regressions were used to estimate the influence of stem density on SDRs, however they were not significant.

Bulk density

Bulk density was not significantly different across the north to south latitudinal gradient of HC but was significantly different along the gradient in KC tidal. KC A bulk density was significantly higher than KC C (ANOVA, F= 5.91, DF=2, P<0.0064, Figure 17). Bulk density was not significantly different across the elevational gradient in either HC or KC tidal but was typically higher in blocks A compared to blocks B and C in both sites. Bulk density was not significantly different between the KC non-tidal transects. Across all three sites, bulk density was significantly higher in KC non-tidal and lowest in HC (ANOVA, F= 19.37, DF=2, P<0.0001, Table 3).

Organic matter content

Organic matter (%O.M.) was not significantly different between the two KC non-tidal transects or across the latitudinal or elevational gradients within either HC or KC tidal.

No significant difference in %O.M. was found between HC and KC tidal however, both HC and KC tidal, had significantly higher %O.M. compared to KC non-tidal (ANOVA, $F= 71.33$, $DF=2$, $P<0.0001$, Table 3).

Stream morphometry of Kimages Creek

The channel gradient was considerably steeper in the non-tidal portion of Kimages Creek than in the tidal portion (Table 4). Width-depth ratios for cross sections in the tidal portion of Kimages Creek were higher than those in the non-tidal, as a result of the widened channel in the tidal section, and a more incised, narrow channel in the non-tidal section. In the non-tidal reach, bank widths averaged 6.31 ± 3.19 m and mean depth was 2.04 ± 0.75 m. However, in the tidal reach, mean bank width was 26.47 ± 6.68 m and average depth was 0.54 ± 0.97 m (Figure 18, Table 4).

Carbon-14 results

The ^{14}C results of the tidal core samples are as follows: sample A, 1990 ± 25 yrs. BP (located 300 cm below surface); sample B, 900 ± 20 yrs. BP (located 140 cm below surface); sample C, 280 ± 20 yrs. BP (located 70 cm below surface). ^{14}C dating resulted in the following ages for the two non-tidal samples: sample A, 890 ± 25 yrs. BP (located 200 cm below surface); sample B, 100 ± 20 yrs. BP (located 120 cm below surface). For the purpose of characterizing sediment within the aged intervals of the cores the following labels will be used for each of the segments: tidal modern, uppermost-youngest segment in the tidal core (between 70-0 cm below sediment surface); tidal relic, deepest-oldest segment of tidal core (between 300-150 cm below sediment surface); non-tidal LS, uppermost-youngest segment in the non-tidal core (between 120-0 cm below sediment surface); and non-tidal relic, deepest-oldest segment of non-tidal core (between 200-130 cm below sediment surface) (Figure 19).

Vertical accretion (VA) rates (mm y^{-1}) and carbon accumulation (CA) rates (g C m^{-2} y^{-1}) were calculated for each core segment. VA rates ranged from 1.43-1.50 mm y^{-1} in the relic tidal segment and from 1.91-2.14 mm y^{-1} in the tidal modern segment. While a minor increase in VA was seen in the tidal core, there was greater than a five-fold increase from relic segment (ranged from 0.98-1.05 mm y^{-1}) to LS segment (ranged from 6.42-8.16 mm y^{-1}) in the non-tidal core (Figure 20). The VA rates of this study are plotted against VA rates found in other tidal freshwater marshes in the mid-Atlantic region, which were calculated using similar dating methods (Figure 25, modified after Neubauer et al*.*, 2002). VA increased at different rates between cores. However, CA rates increased from the relic segments to the LS/modern segments by similar amounts. CA rates in the tidal relic segment ranged from 143.75-150.50 g C m^{-2} y^{-1} and increased to 380.62-427.18 g C m^{-2} y^{-1} in the tidal modern segment. In the non-tidal core, CA rates increased from a range of 130.14-138.64 g C m^{-2} y^{-1} in the relic sediment to 418.59-532.49 g C m^{-2} y^{-1} in the LS segment (Figure 21).

<u>Within core characterization</u>

A series of paired-t-tests were performed within cores for the following: bulk density, %O.M., %carbon, %nitrogen, C/N ratios (molar), and CIA values. In the non-tidal core, %C, and %O.M. were statistically significantly lower in the LS segments compared to the relic sediment (%C: paired *t*-test, p=0.0009*;* %O.M.: Wilcoxon signed rank test, p=0.0273, Figure 22, Table 5).

C: N molar ratios were also significantly lower in the LS segment compared to the non-tidal relic segment (Wilcoxon signed rank test, p=0.0078, Table 6). The CIA values (calculated via equation 1) were significantly different between the relic (66.36 ± 0.73) and LS segments (72.65 ± 0.95) of the non-tidal core with a higher average CIA found in the LS segment indicating greater weathering (paired t-test, p=0.0002, Table 6). In the tidal core, the modern sediment segment had significantly higher %C compared to the relic segment (12.83 ± 8.95% vs. 6.64 ± 6.61%; paired t-test, p=0.0383, Figure 23, Table 5) however, no other significant differences (CIA, %O.M., %N, C: N molar ratios) were found.

Between core characterization

A series of t-test were performed between cores comparing the tidal modern segment to the non-tidal LS segment and the tidal relic segment against the non-tidal relic segment for the following: bulk density, %O.M., %carbon, %nitrogen, C/N ratios (molar), and CIA values. Bulk density in the non-tidal LS and non-tidal relic segments were significantly higher than in the tidal modern and tidal relic segments (LS vs. modern, Wilcoxon test p=0.0112, Table 6*;* relic vs. relic, t-test p<0.0001). %C and %O.M. were significantly lower in the non-tidal LS segment compared to the tidal modern segment (% C t-test p=0.0147, *%O.M.* t-test p=0.0101, Table 5, Figures 22 and 23). Similarly, the non-tidal relic segment had significantly lower %C and %O.M. than the tidal relic segment (% C t-test p=0.0096, *%O.M.* t-test p=0.0012, Table 5, Figures 22 and 23). C: N molar ratios were significantly lower in the non-tidal LS segment compared to the tidal modern segment (t-test p=0.0036). No significant difference in C: N molar ratios were found between the two relic segments between cores. CIA was significantly lower in the non-tidal relic segment than in the tidal relic segment (t-test p=0.0739, Table 6). However, no significant difference in CIA was found between the tidal modern and non-tidal LS segments or between the tidal modern segment and the tidal relic segment.

Elevation change over time

Using the known vertical elevation measurements (NAVD 88, Geoid 12b) at the surface of both core locations, vertical elevation of the tidal ^{14}C sample B, 900 ± 20 yrs. BP (located 140 cm below surface) and vertical elevation of the non-tidal ^{14}C sample A, 890 ± 25 yrs. BP (located 200 cm below surface) were determined. With the known elevation and distance between cores (1,044.56 m), the slope (m/m) was calculated for the current surface and between sample B in the tidal core and sample A (Figure 24). Historically, the difference in elevation between the non-tidal sample A (-0.761 m) and tidal sample B (-1.507 m) is 0.746 m, equaling a slope of 0.0007. Comparatively, the current elevation difference between the non-tidal core surface (1.239 m) and the surface of the tidal core (-0.1707 m) is 1.4097 m, resulting in a slope, (0.0014), that is 1.89 times steeper than historical measures.

Core descriptions: color and organic/inorganic material presence

Within the tidal relic segment, color shifted from the bottom up as follows: greenish gray (5 G 6/1), grayish brown (2.5Y 5/2), very dark gray (2.5Y 3/1), black (2.5Y 2/5.1), very dark gray (10YR 3/1). Considerable amounts of woody debris and leaf material were found between 230-190 cm below surface as well as a 5 cm layer of gravel around 270 cm below surface. Color changed up the tidal modern segment from dark brown (10YR 3/3) to very dark gray (10YR

3/1). Woody fragments were observed between 50-20 cm below sediment surface along with a densely fibrous root layer just below sediment surface.

The relic segment in the non-tidal core shifted from dark gray (10YR 4/1) to very dark gray (10YR 3/1) and then to black (10YR 2/1) up the core. Considerably large amounts of woody fragments and leaf material were observed between 200-135 cm below surface with very well preserved *Alnus serrulata* seed cones found between 180-175 cm below surface. Significant amounts of course sand and gravel were found at the very bottom of the core suggesting the presence of a historic stream channel point-bar. The non-tidal LS segment was primarily gray (5Y 5/1) and olive gray (5Y 4/2) with a slight shift to dark brown (10YR 3/3) at the top of the core. Some leaf material was found around 80 cm below surface but little woody debris was found within the LS core segment.

Discussion

Current temporal and spatial variations in sediment deposition

The results of this study revealed substantial spatial variability in SDRs within every site however, the mechanisms governing this apparent variation might be slightly different for each of the three sites. Harris Creek, a forested system with associated hummocks and hallows, contained the most microtopography. Kimages Creek had the widest floodplains with SCTs spread across a greater distance from creek bank to toe of slope. KC non-tidal has floodplain widths similar to HC while containing much less microtopography. However, KC non-tidal was the only site that was repeatedly impacted by the presence of beaver activity throughout the sampling period. This resulted in changes in hydrologic connectivity throughout the non-tidal floodplains with the rise and fall of several beaver dams, which altered patterns of sediment deposition sporadically.

Temporal variation within the sampling period was observed across all transects with significantly higher rates of sediment deposition occurring during the growing season. While vegetation had a minor influence on SDRs, precipitation patterns explained a higher percentage of the variation on SDRs across the tidal transects (Figures 14-16). In particular, highest average monthly SDRs were measured in May 2016, which was not only the wettest month in the sampling period but the wettest May recorded since 1889, according to the National Weather Service (Figures 12 and 13). Therefore, the significant difference in SDRs between growing season and non-growing season may be due to the irregularly high rainfall events observed in

May 2016 and might not be indicative of temporal variations in SDRs outside of this sampling period.

In a study of sediment deposition in a mid-Atlantic tidal freshwater marsh by Neubauer et al., (2002) average SDRs ranged from 56.5 to 284.2 g sediment m^{-2} d^{-1} with highest SDRs found at the creek bank locations compared to marsh interior or toe of slope locations. Similar average SDRs ranges and spatial patterns were observed in this study as higher rates of sediment deposition occurred on SCTs situated at the creek bank. This depositional pattern is a function of settling and flow velocities where high velocities quickly dissipate as flow reaches the topographically elevated stream banks, allowing for heavier sediments to fall out of suspension (French and Spencer, 1993; Esselink et al., 1998; Neubauer et al., 2002; Hupp et al., 2013). Secondly, as the floodwater makes its way into the interior of the floodplain, velocity is further slowed and sediments are continually being deposited. This may also support the lack of influence stem density had on sedimentation rates as compared to the effect of the elevational gradient.

No significant differences in SDRs were observed between HC, the reference natural site, and the KC tidal site. This suggests the prior land use modifications of impoundment have not significantly altered the reestablished tidal floodplains' ability to retain sediment. Relative to the non-tidal transects, the tidal transects had significantly higher SDRs, as deposition is largely influenced by distance to the primary sediment source coupled with floodplain connectivity, which impacts levels of inundation. While the linear distance to sediment source was similar between the non-tidal and tidal transects, the non-tidal floodplain does not receive tidal subsidies and exhibits less hydrologic connectivity as that reach of KC is more incised. Sediment deposition has a direct impact on accretion rates and accretion can in turn impact deposition through altering the duration and frequency of inundation (Neubauer et al., 2002, Hedges and Keil, 1995). This interaction may be, in part, what is driving the current low rates of deposition observed in non-tidal floodplains as accretion rates, calculated via carbon dating of soil cores, were substantially higher than what was found in the tidal core.

Additionally, the significant differences in O.M. content between the tidal and non-tidal transects are reflected in the sediment core results and are most likely driven by the absence of tidal subsidies and presence of less labile vegetation in the non-tidal floodplains. Bulk density was commonly higher in the non-tidal transects relative to the tidal floodplains and significantly higher compared to HC transects. The difference in bulk density between the tidal and non-tidal floodplains was also mirrored in the results found in the sediment cores and may be due in part to the presence of coarse grain LS deposited within the non-tidal floodplains. The general trend of higher bulk density found in blocks A (near creek banks), where flow velocities tend to be the highest as it intercepts the elevated stream banks, allows for the coarse-grained mineral deposition (Neubauer et al. 2002, Hupp et al. 2013).

Characterization of legacy sediment and relic hydric sediment

While visual and textural identification of LS has been sufficiently established in research performed throughout the Mid-Atlantic Piedmont region, no studies have focused on low-gradient Coast Plain systems. Therefore, visual and textural identification methods previously used are neither applicable nor sufficient enough to determine the presence or absence of LS at this site. One of the primary objectives of this study was to characterize and identify the presence or absence of LS as it exists within a tidal and a non-tidal Coastal Plain stream and floodplains. To accomplish this, ^{14}C dating was used to establish aged segments of sediment cores from the tidal and non-tidal floodplains of Kimages Creek and multiple analyses of sediment characterization were conducted to compare segments within and between cores.

Substantial differences in VA rates were observed between the relic non-tidal compared to the LS non-tidal segment however, very little difference was observed within the tidal core between the relic and modern segments. The rate of accretion in the LS non-tidal segment is also substantially higher than what was calculated across the tidal core. Moreover, differences in VA rates between the tidal core segment and the non-tidal relic segment were minor. Decreased rates of accretion with increased time scales have been observed across multiple studies (e.g. McKee et al., 1983: Neubauer et al., 2002), which suggest the mechanisms for the observed reductions in VA could be a combination of greater compaction, inclusion of storm-induced erosion events, and metabolism of labile sediment. However, those impacts would affect the entire site and therefore do not fully explain the observed decrease in VA over time as only one core (non-tidal) showed substantial differences in rates. This suggests a considerable deposition event occurred primarily in the non-tidal portion of KC within the time frame that the damming took place.

While there was a concurrent increase in CA rates in both cores between the relic sections and their corresponding LS or modern segments, the carbon content was not the apparent driver in the non-tidal core. In the tidal core, the modern segment had significantly higher %C than the relic segment which helps explain the increase in CA rates observed. However, in the non-tidal core, %C was significantly lower in the LS segment than in the relic segment, suggesting the increase in CA for the non-tidal core was due to the significant increase in VA.

Within the tidal core, the only measured differences between the modern and relic segments was the increase in %C. The significantly higher %C in the modern segment may be due in part to metabolism of labile sediment fractions in the relic segment in conjunction with the current deposition of organic content from herbaceous vegetation within the root zone and increased anoxic conditions during impoundment in the modern segment. Comparatively, in the non-tidal core, %C, %O.M. and C/N ratios (molar) were all significantly lower in the LS segment versus the relic section. This reduction in carbon and organic matter content is also visually prominent through the color shift within the non-tidal core between the relic and LS segments.

As tidal sediments are exposed to incoming and outgoing tidal forces twice a day at this site, it is expected to find higher levels of weathering in a tidal rather than non-tidal regime. Our results supported this generalization in the relic sediments as CIA values were significantly higher in the relic tidal compared to the relic non-tidal segment; however, there was no significant difference in CIA between the tidal modern and non-tidal LS segments. This pattern would also be expected in legacy sediments as they persisted in a very different depositional environment relative to the historic non-tidal or tidal freshwater-forested wetlands. Therefore, significant differences between non-tidal LS and non-tidal relic segments would also be expected. If LS were deposited evenly across the reservoir (tidal and non-tidal), a significant difference in CIA between the tidal segments would be anticipated yet no difference was observed.

The measure of slope from the surface of the non-tidal core to the surface of the tidal core was roughly twice as steep as the slope calculated from measured elevations at ^{14}C markers that designate relic wetland surfaces. This elevational shift demonstrates the significant increase in vertical elevation of the non-tidal floodplain relative to the floodplain in the tidal wetlands. Further suggesting legacy sediment deposition occurred primarily in the non-tidal portion of KC while, in the tidal portion, modern hydrology and sedimentation post dam removal was not substantially altered from pre-impoundment conditions.

Current research at milldam sites shows LS deposition increases with proximity to the dam as does stream bank erosion and stream incision after dam breaching (Merritts et al. 2011). However, in this low-gradient coastal plain stream, the relationship between LS deposition and subsequent incision and erosion seems to be reversed with maximum LS deposition, stream incision and bank erosion occurring furthest from the dam. This shift in LS deposition is potentially a function of valley gradient impacting settling and flow velocities. Therefore, channel evolution models, aimed at understanding channel shifts post dam removal (like that proposed by Doyle et al., 2002), which may be applicable across a majority of moderate to high gradient fluvial systems might be inappropriate in a low-gradient Coastal Plain site. Additionally, the current restoration management technique of LS removal in dam-impacted sites within the Piedmont region may not be necessary or even beneficial in these lower gradient systems.

The portion of the former lake basin that contains LS has the potential to transition to a sediment source for the rest of the site downstream. In previous studies of dam removal, the transition of LS from a sink to a sediment source has been considered a negative result of impoundment as excessive sedimentation has caused adverse impacts on downstream biota (Stoker and Harbor, 1991: Beck, inc., 1998). However, within the KC tidal wetland restoration, LS may increase sediment accretion and increase the survivability of these wetlands as sea levels rise.

The results from radiocarbon dating indicate VA rates in the relic and modern sediments of the tidal core are comparable to rates found in other tidal salt and freshwater marshes in the mid-Atlantic region (Figure 25). Although, the rates of vertical accretion in the modern tidal segment have slightly exceeded observed values from the tidal benchmark (relic hydric segment), they are still relatively low compared to the estimated RSLR rate of Virginia (4.25 ± 0.23 mm y^{-1}) (Boon, 2005). Therefore, utilization of existing LS, rather than removal, could make restoration of streams and wetlands in low-gradient regions more advantageous. Particularly for sites within the Chesapeake Bay watershed where tributaries have shown declines in suspended-sediment concentrations (Weston, 2014), and where rates of RSLR are suggested to be greater than global averages (Sallenger et al., 2012).

Conclusions

Current temporal and spatial variations in sediment deposition

In the tidal reaches of Kimages and Harris Creek, the greatest rates of sediment deposition occurred closest to creek banks indicating tidal influence and duration of inundation are strong drivers in sediment deposition at these sites. Parallel spatial deposition patterns along elevational gradients coupled with similar SDRs between HC and KC tidal suggest sediment deposition within KC is similar to sediment deposition in HC, thus hydrologic connectivity of the KC tidal floodplain maybe approaching functional equivalency with the reference site. The significantly lower rates of sedimentation deposition in the non-tidal reach of Kimages may be due to the lack of tidal subsidies coupled with a lack of floodplain connectivity due to greater stream incision compared to the tidal transects. The considerable stream incision in the non-tidal floodplains resulting in decreased hydrologic connectivity might be a result of the LS deposition during impoundment. While sedimentation rates were highly variable within and across transects, sediment deposition tended to follow precipitation patterns closely. The largest spike in sediment deposition across all transects occurred during May 2016, which corresponds to the wettest month during the sampling period and wettest May on record.

Characterization of legacy sediments and relic hydric sediments

Rates of accretion and carbon accumulation of the tidal modern segment have either reached or exceeded that of the tidal benchmark (relic hydric segment), which is a positive outcome for a restored system. However, vertical accretion rates of both the benchmark and modern tidal segments are not sufficient enough to maintain positive surface elevation relative to the estimated RSLR rate of Norfolk, Virginia (4.25 ± 0.23 mm y^{-1}) (Boon, 2005). Therefore, the potential transport of the stored LS in the non-tidal floodplains may become a vital source of sediment for these restored tidal wetlands.

In dam-impacted streams within the Piedmont region, the LS accumulation and stream incision increased with proximity to the dam, which has resulted in decreased floodplain connectivity. The increase in floodplain surface elevation in these systems has prompted the removal of LS in restoration projects to restore the naturally occurring, buried riparian wetlands (Merritts et al. 2011). However, within this low-gradient coastal plain stream the opposite pattern of LS accumulation and stream incision was observed. Our results suggest that in coastal plain streams impacted by dams, the subsequent LS may become a benefit rather than a liability for downstream tidal wetlands.

As funding and resources for tidal wetland restoration is limited it is imperative to understand how different land use modifications (impoundment, clear cutting, and agricultural draining,) impact the rate at which natural functioning is restored to these systems. Results from this study show rates of accretion and carbon accumulation have met or exceed that of the benchmark rates determined from the ^{14}C. Current rates of sediment deposition are similar to the natural reference site, HC. These findings suggest wetland restoration via dam removal in low gradient Coastal Plain systems may be more advantageous compared to dam-removal restoration projects in higher gradient regions; and potentially more successful in terms of vertical accretion, carbon accumulation, and sediment deposition compared to other types of restoration efforts (i.e. sites being restored after agricultural draining) in lower gradient coastal plain regions.

Tables and Figures

Table 1. Average sediment deposition rates of growing season and non-growing season across all sites. Values are means ± 1 standard error.

Site	Growing Season SDRs	Non-Growing season SDRs
Harris Creek	84.87 ± 16.86	44.94 ± 11.66
Kimages Creek Tidal	98.92 ± 23.08	56.52 ± 11.77
Kimages Creek Non-tidal	26.08 ± 7.84	11.68 ± 4.12

Table 2. Average stem count per transect during peak growing season and during middle of non-growing season. Values are means ± 1 standard deviation.

Transect	Growing Season	Non-growing Season
HCA	131.00 ± 69.07	130.33 ± 96.21
HCB	304.33 ± 239.54	208.67 ± 136.67
HCC	170.00 ± 77.62	130.33 ± 51.78
KCA	327.67 ± 65.74	146.33 ± 165.62
KCB	263.33 ± 18.92	219.33 ± 154.08
KCC	328.33 ± 65.31	222.30 ± 65.45
NTA	381.00 ± 98.98	526.51 ± 33.23
NTB	422.50 ± 26.35	469.01 ± 117.38

Table 3. Average bulk density and organic matter content across all sites. Values are means ± 1 standard error. Lower case letters indicate significant differences among sites $p<0.05$.

Site	%O.M.	Bulk density (g sediment cm^{-3})
Harris Creek	23.27 ± 0.46 [a]	0.377 ± 0.006 [a]
Kimages Creek Tidal	22.17 ± 0.46 [a]	0.408 ± 0.006 [a]
Kimages Creek Non-tidal	13.78 ± 0.46 [b]	0.432 ± 0.007 [b]

Table 4. Stream morphometry for Kimages Creek. Values for channel gradient, bank width, and mean depth are means ± 1 standard deviation.

Reach	Sinuosity	Channel Gradient (cm/m)	Bank widths (m)	Mean depth (m)	Width/depth ratio
Non-tidal	1.03	0.6503 ± 0.89	6.37 ± 3.19	2.04 ± 0.75	3.13
Tidal	1.02	0.0196 ± 0.10	26.44 ± 17.68	0.54 ± 0.97	48.52

Table 5. Mean values of organic matter content (%O.M.) and total carbon (%C) for each core segment. Values are means ± 1 standard error. Lower case letters indicate significant differences within cores (paired *t*-tests: non-tidal LS vs. non-tidal relic segment and tidal modern and tidal relic segment) $p<0.05$. (+) indicates significant differences between cores (*t*-tests: non-tidal LS vs. tidal modern segment and non-tidal relic vs. tidal relic segment) $p<0.05$.

Core Segment	%O.M.	%C
Non-tidal LS	$3.08 \pm 0.52^{a, +}$	$1.39 \pm 0.33^{a, +}$
Non-tidal relic	$3.87 \pm 0.53^{b, +}$	$2.17 \pm 0.13^{b, +}$
Tidal modern	$25.63 \pm 6.1^{+}$	$12.83 \pm 3.38^{a, +}$
Tidal relic	$14.84 \pm 2.73^{+}$	$6.64 \pm 1.5^{b, +}$

Table 6. Mean values of bulk density, C/N ratio (molar), and Chemical Index of Alteration (CIA) for each core segment. Values are means ± 1 standard error. Lower case letters indicate significant differences within cores (paired *t*-tests: non-tidal LS vs. non-tidal relic segment and tidal modern and tidal relic segment) $p<0.05$. (+) indicates significant differences between cores (*t*-tests: non-tidal LS vs. tidal modern segment and non-tidal relic vs. tidal relic segment) $p<0.05$.

Core Segment	Bulk density (g sediment cm^{-3})	C/N ratio (molar)	Chemical Index of Alteration (CIA)
Non-tidal LS	$1.01 \pm 0.08^{+}$	$9.86 \pm 1.56^{a, +}$	72.65 ± 0.95^{a}
Non-tidal relic	$1.21 \pm 0.07^{+}$	19.99 ± 2.01^{b}	$66.36 \pm 0.73^{b, +}$
Tidal modern	$0.59 \pm 0.11^{+}$	$19.84 \pm 2.81^{+}$	75.87 ± 1.14
Tidal relic	$0.53 \pm 0.09^{+}$	16.24 ± 1.54	$75.70 \pm 0.66^{+}$

Figure 1. Map of VCU Rice Rivers Center (RRC). Inset map: Location of RRC within Virginia.

Figure 2. Kimages Creek Wetland Restoration. Pre-restoration (upper left): Impoundment of KC, former Lake Charles. Transitional (upper right): partial breach (occurred in 2006) photo taken in 2007. Restored (lower): partial removal of dam in 2010. By Bukaveckas and Wood, 2014

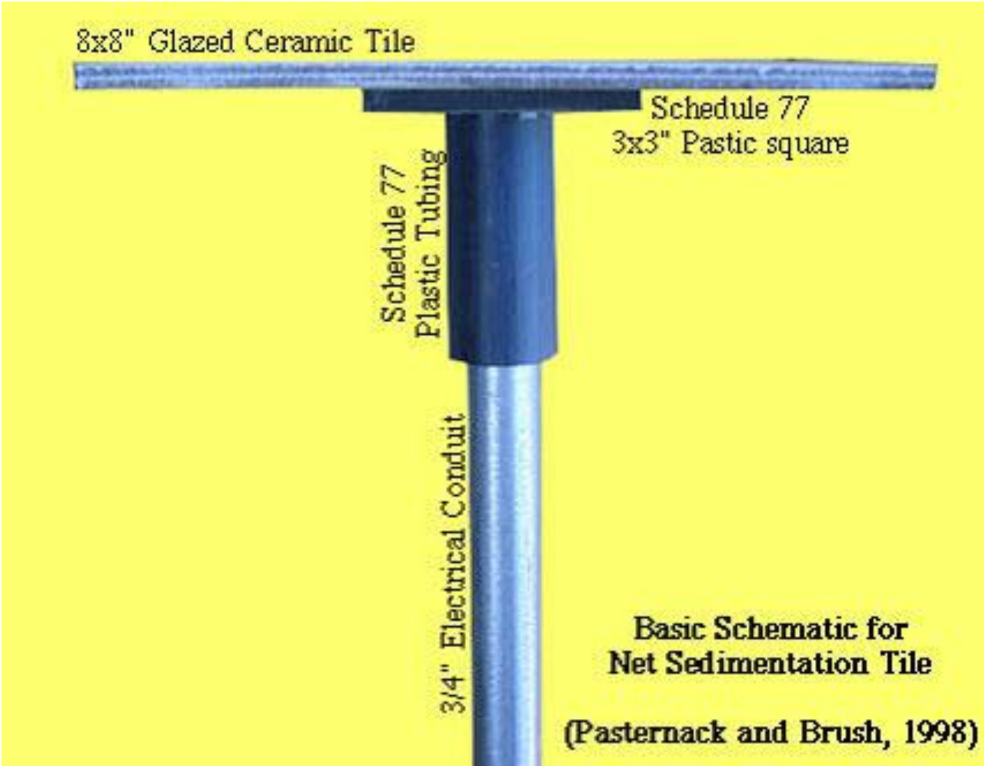

Figure 3. Sediment collection tile schematic by Pasternack and Brush, 1998

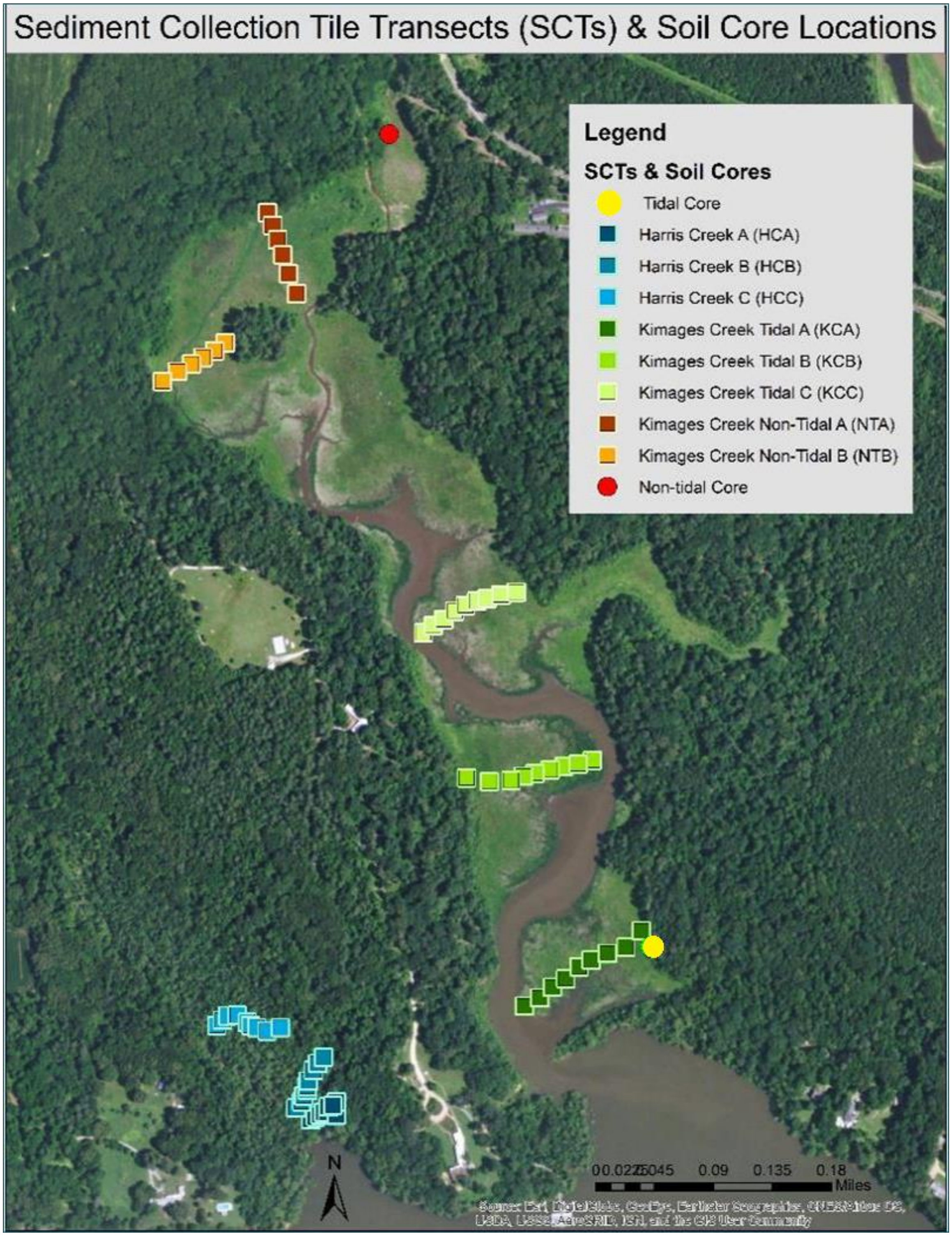

Figure 4. Map of sediment collection tile transects within Kimages and Harris Creek wetlands along with locations of soil cores taken in the tidal and non-tidal portions of Kimages Creek.

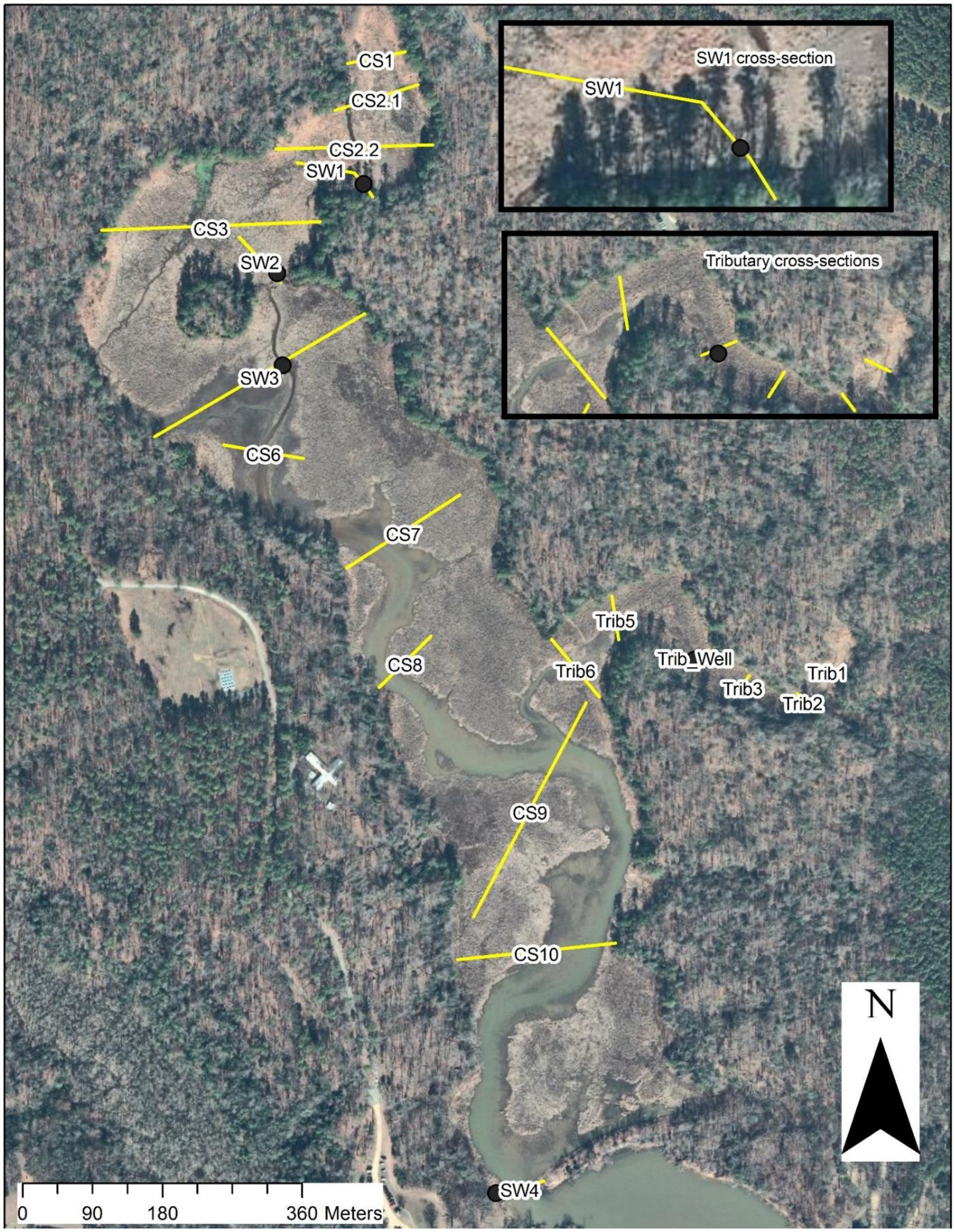

Figure 5: Map of stream monitoring sites along Kimages Creek and a tributary stream. Yellow lines indicate stream and floodplain cross-sections and closed circles indicate cross-section locations with water level loggers. Inset figures show Stream Well 1 and Tributary stream cross-sections.

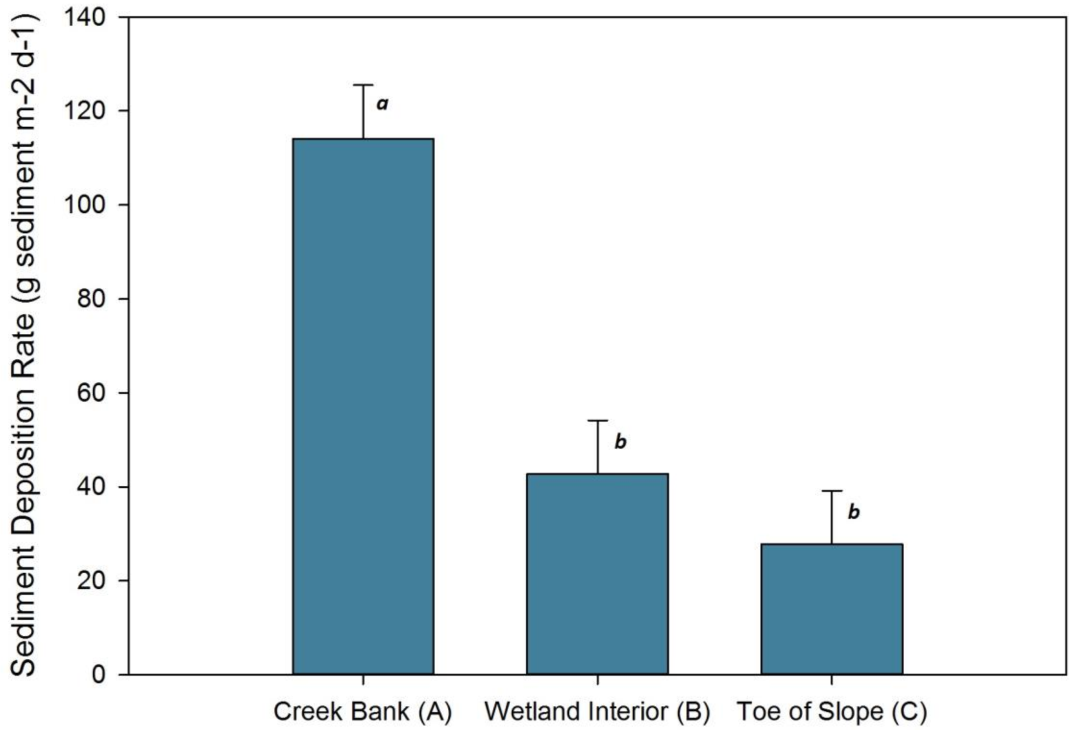

Figure 6. Average Sediment Deposition Rates for each block in Harris Creek. Data presented are means ± Standard error. Lower case letters indicate significant differences among sites $p<0.05$.

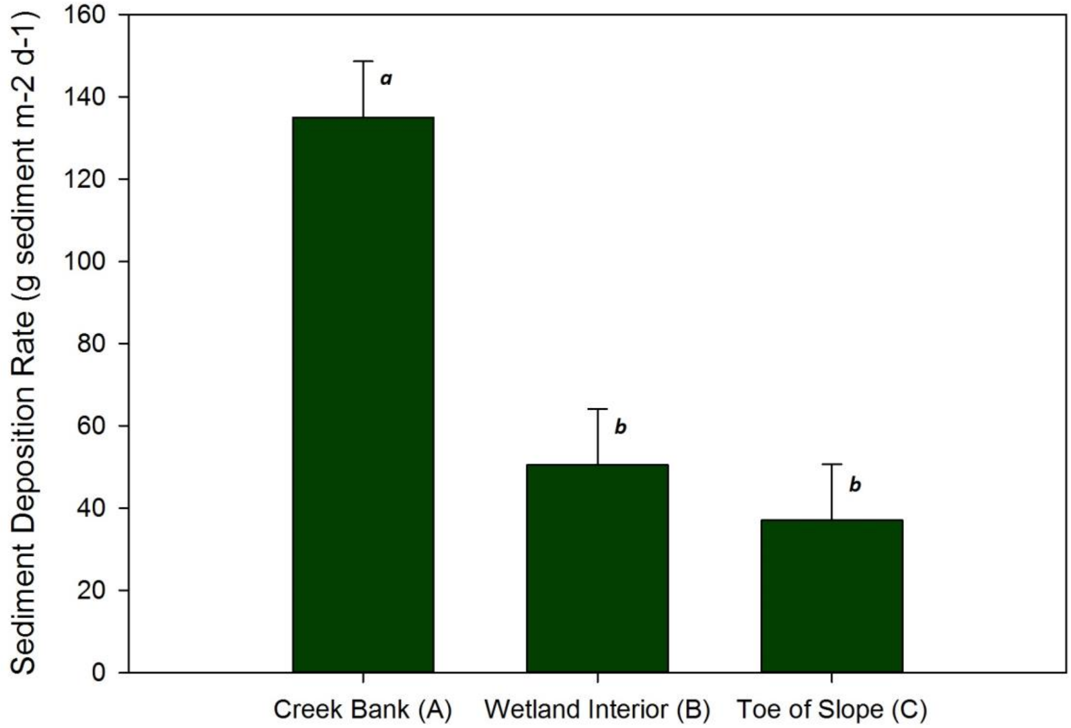

Figure 7. Average Sediment Deposition Rates for each block in Kimages Creek. Data presented are means ± Standard error. Lower case letters indicate significant differences among sites $p<0.05$.

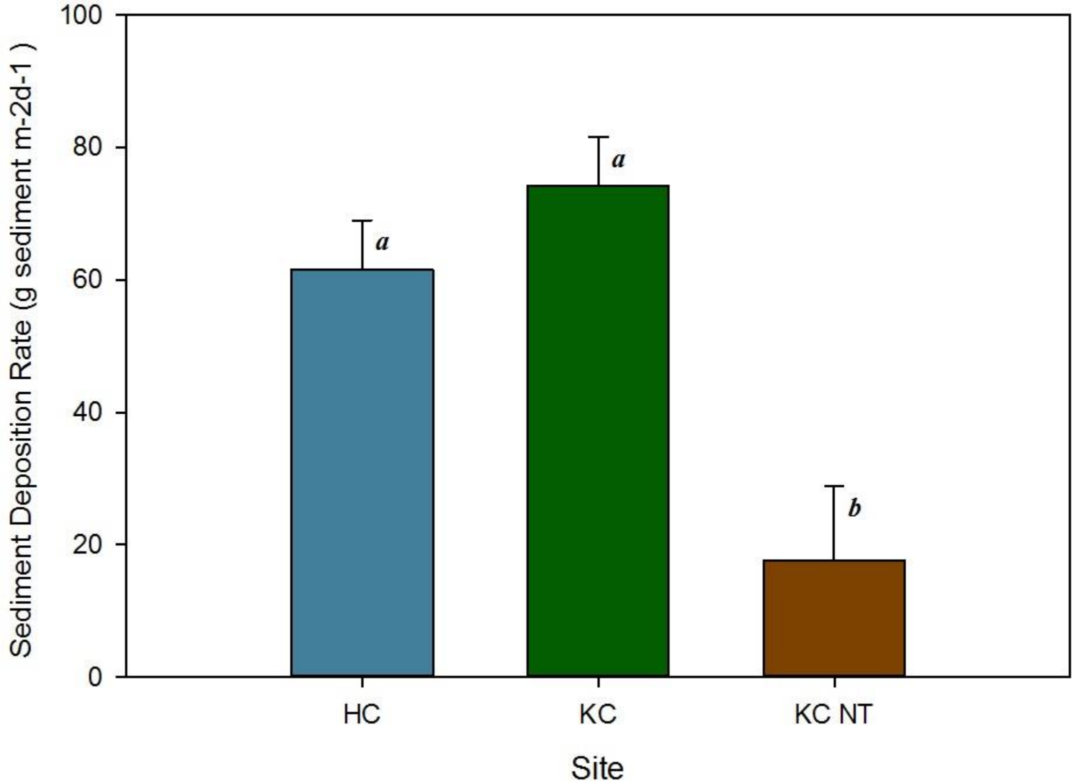

Figure 8. Average Sediment Deposition Rates for each site. Data presented are means ± Standard error. Lower case letters indicate significant differences among sites *p*<0.05.

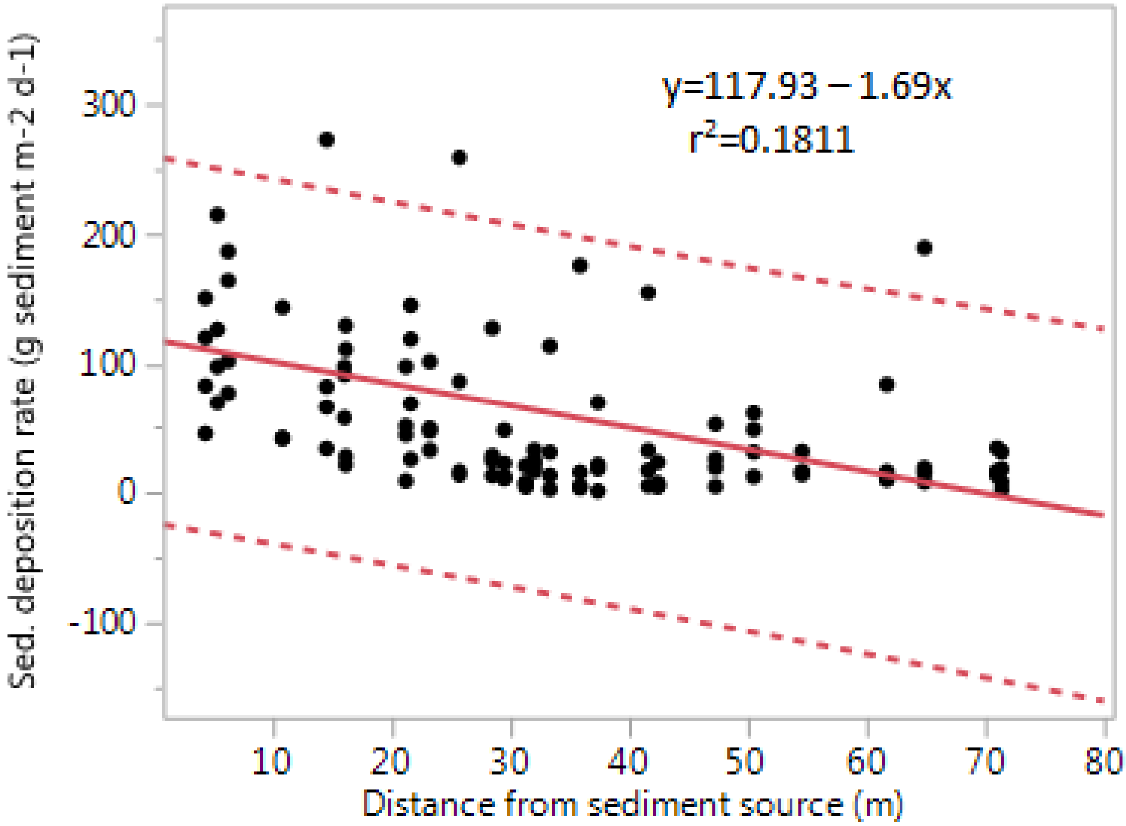

Figure 9. Simple Linear Regression between sediment deposition rates and distance from sediment source for all Harris Creek SCTs. Red dashed line represents prediction interval.

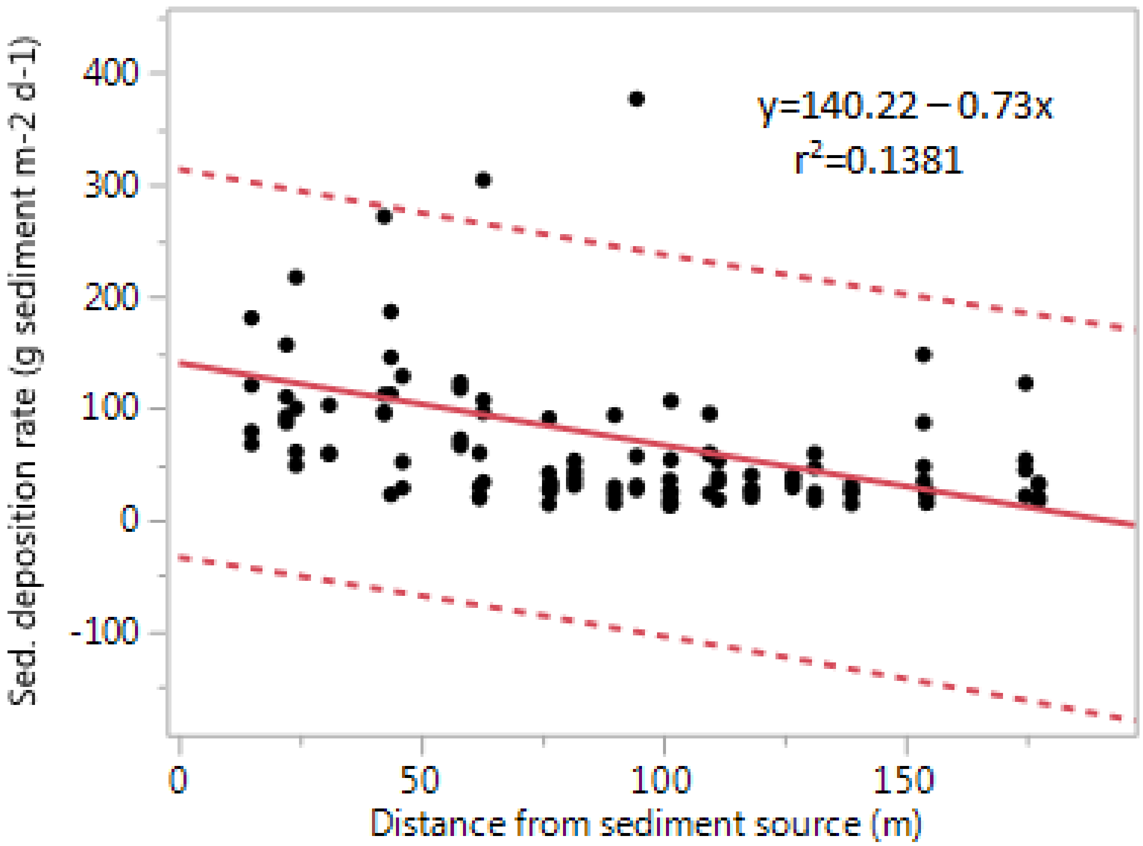

Figure 10. Simple Linear Regression between sediment deposition rates and distance from sediment source for all Kimages Creek tidal SCTs. Red dashed line represents prediction interval.

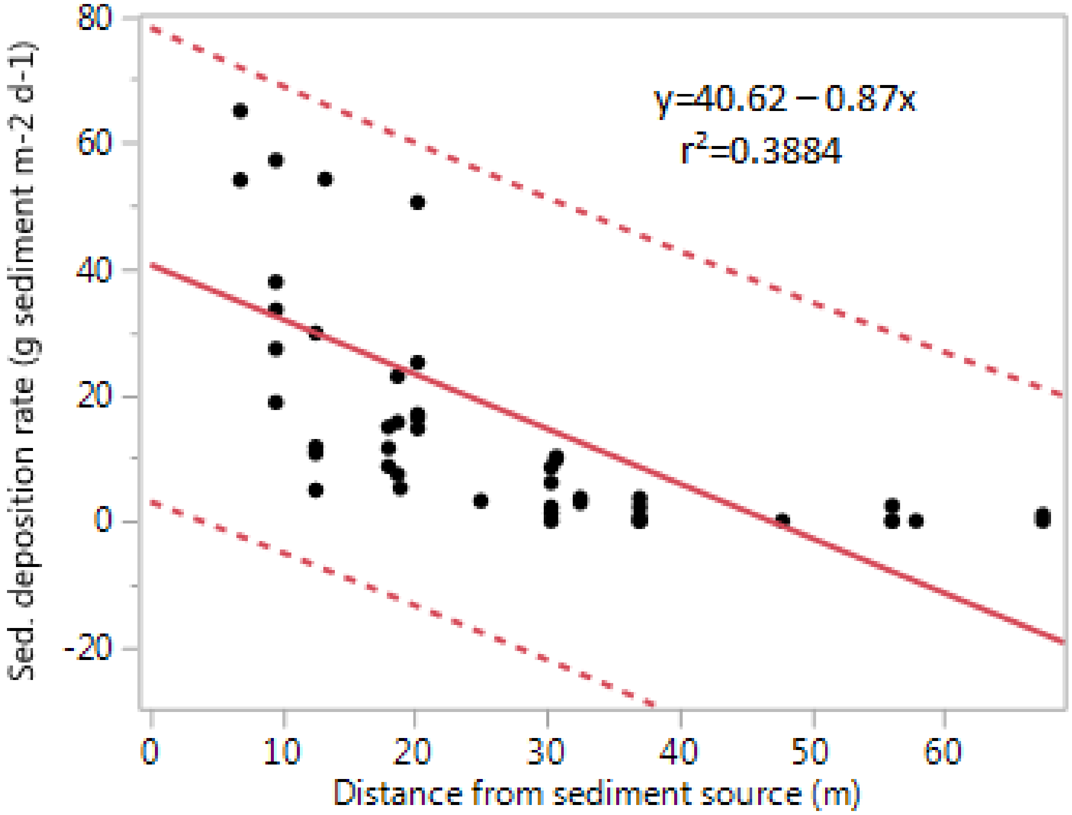

Figure 11. Simple Linear Regression between sediment deposition rates and distance from sediment source for all Kimages Creek non-tidal SCTs. Red dashed line represents prediction interval.

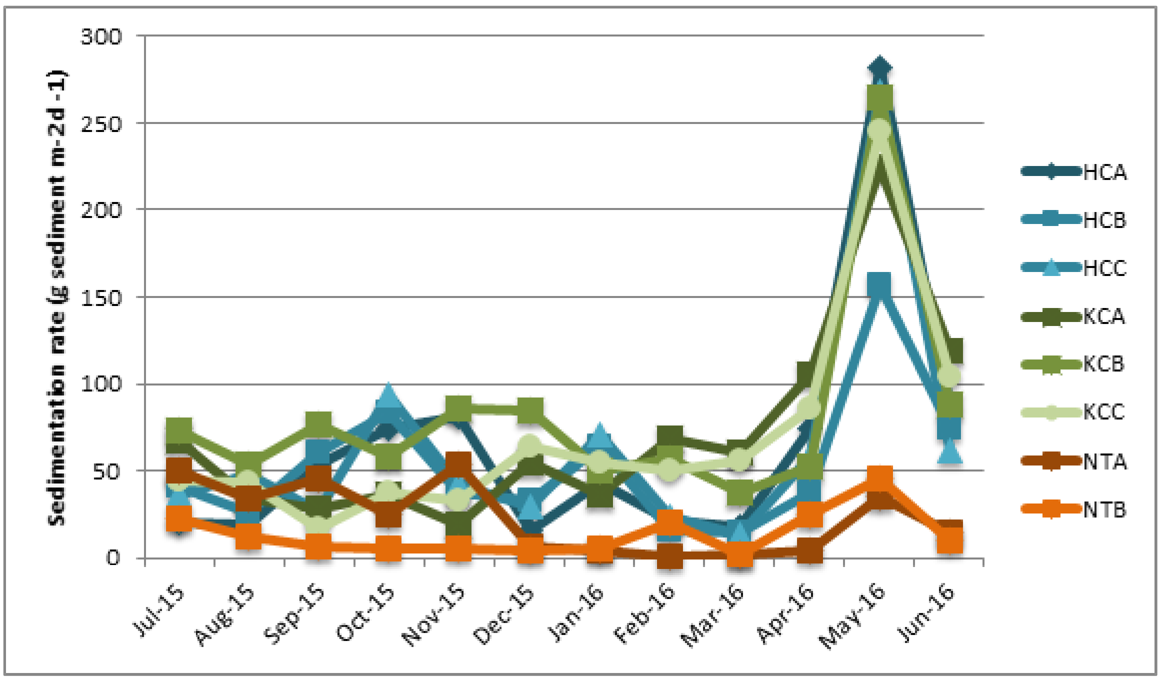

Figure 12. Average sediment deposition rates per month from July 2015 to June 2016 for all transect. Data represents transect means with ranges omitted for clarity.

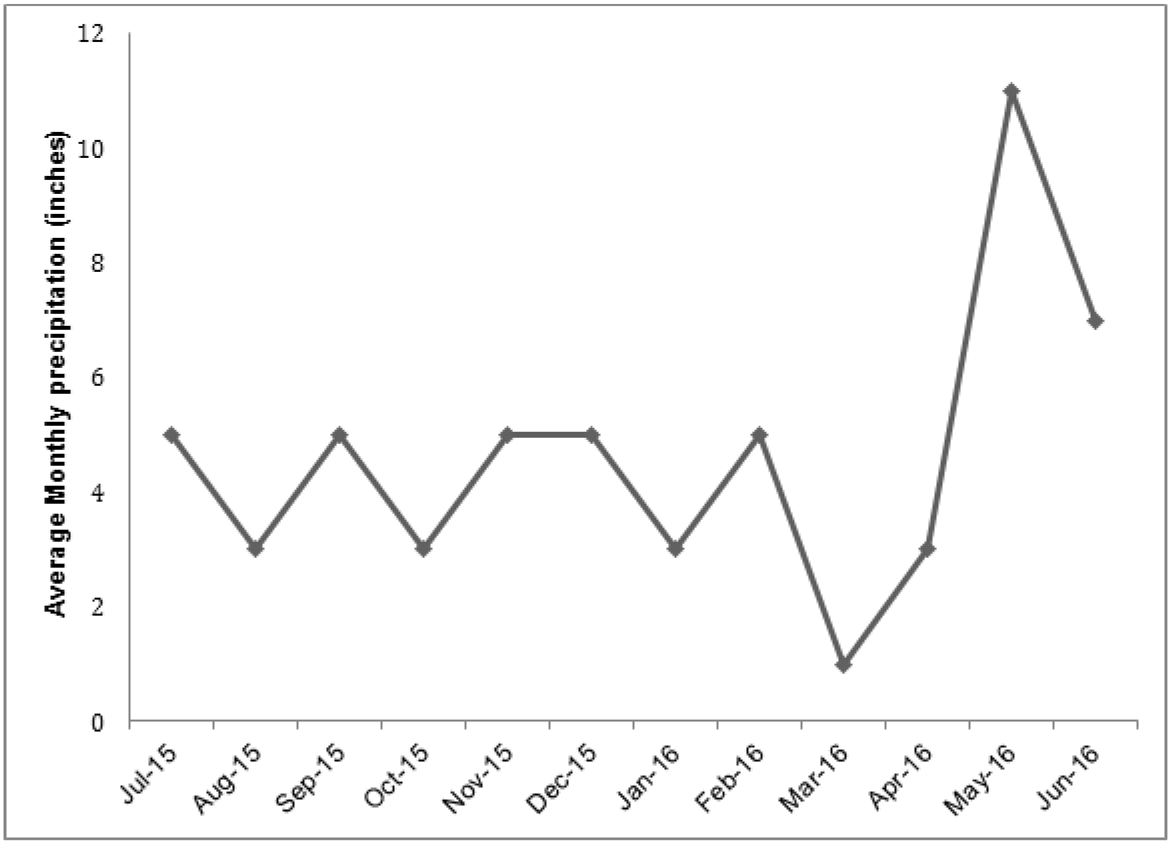

Figure 13. Average precipitation (inches) per month from July 2015 to June 2016 for Hopewell, Virginia. US Climate Data, (2017) *Retrieved January 20, 2017, from* *http://www.usclimatedata.com/climate/hopewell/virginia/united-states/usva0370*

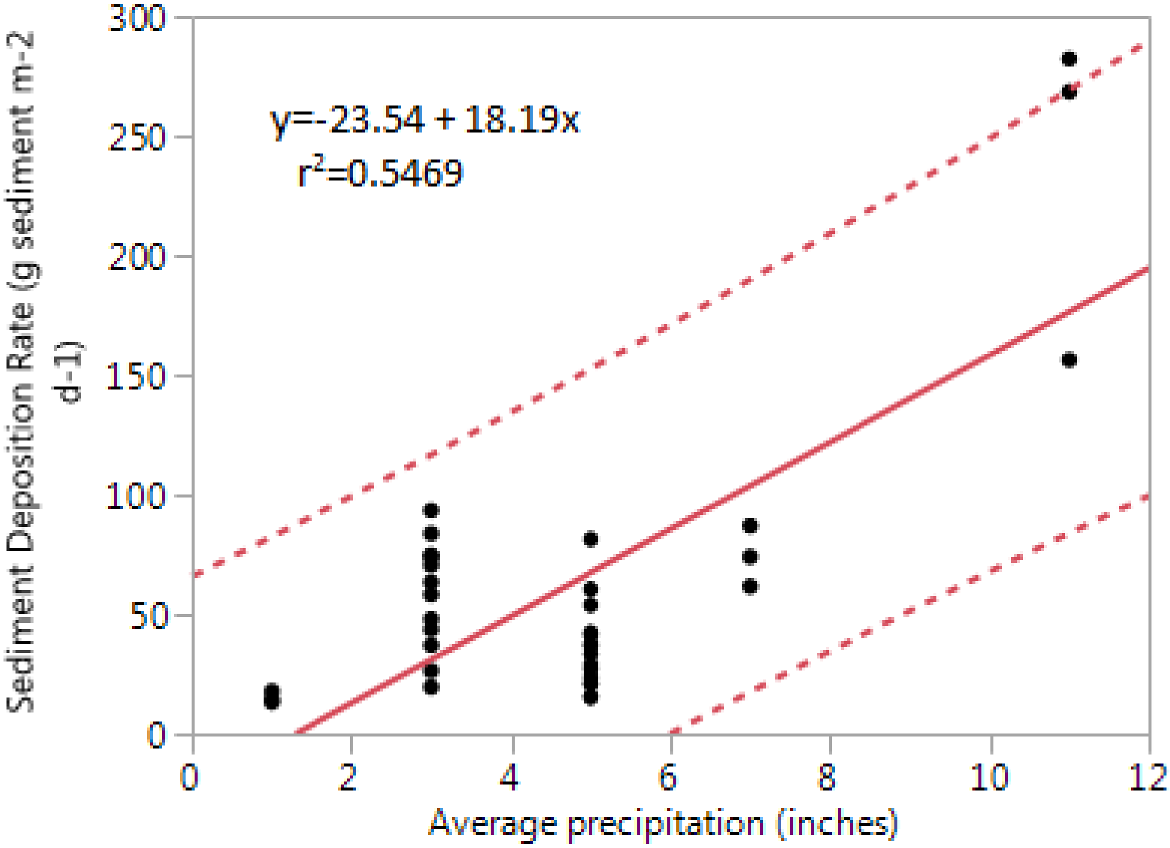

Figure 14. Simple Linear Regression between average sediment deposition rates of Harris Creek and average monthly precipitation (inches) in Charles City County, Virginia. Red dashed line represents prediction interval.

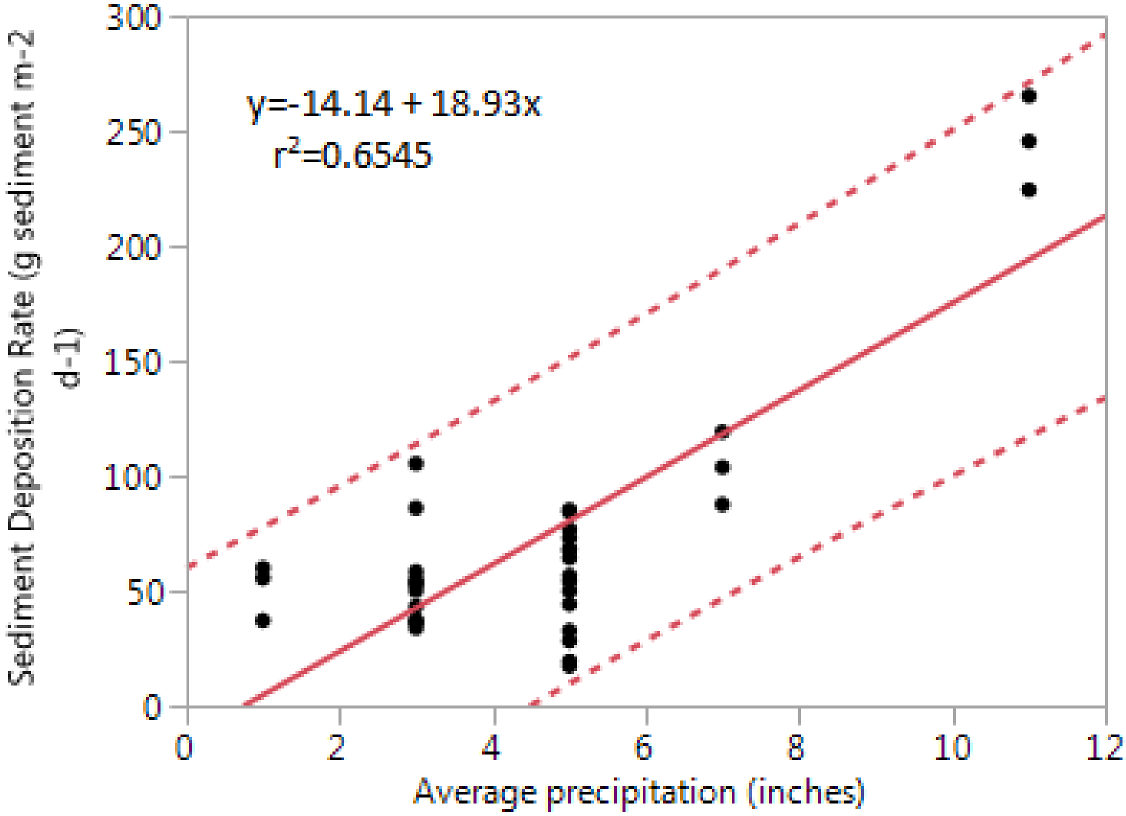

Figure 15. Simple Linear Regression between average sediment deposition rates of Kimages Creek tidal and average monthly precipitation (inches) in Charles City County, Virginia. Red dashed line represents prediction interval.

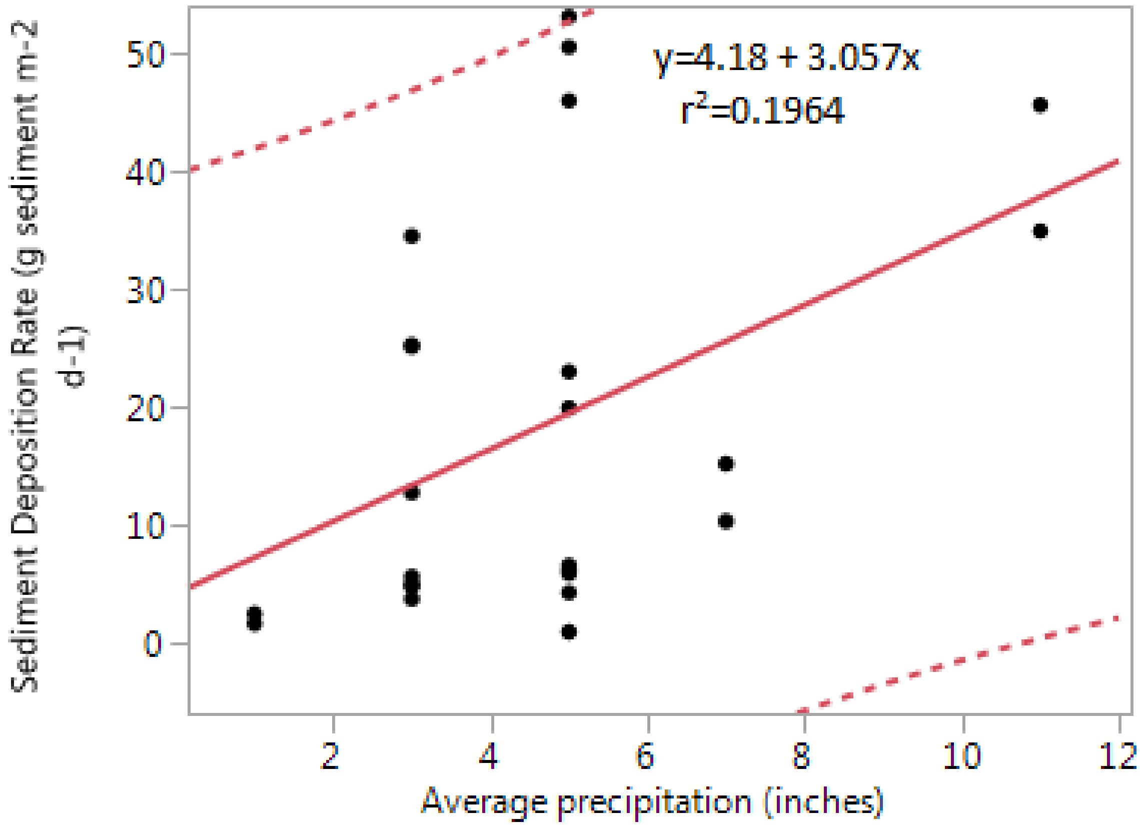

Figure 16: Simple Linear Regression between average sediment deposition rates of Kimages Creek non-tidal and average monthly precipitation (inches) in Charles City County, Virginia. Red dashed line represents prediction interval.

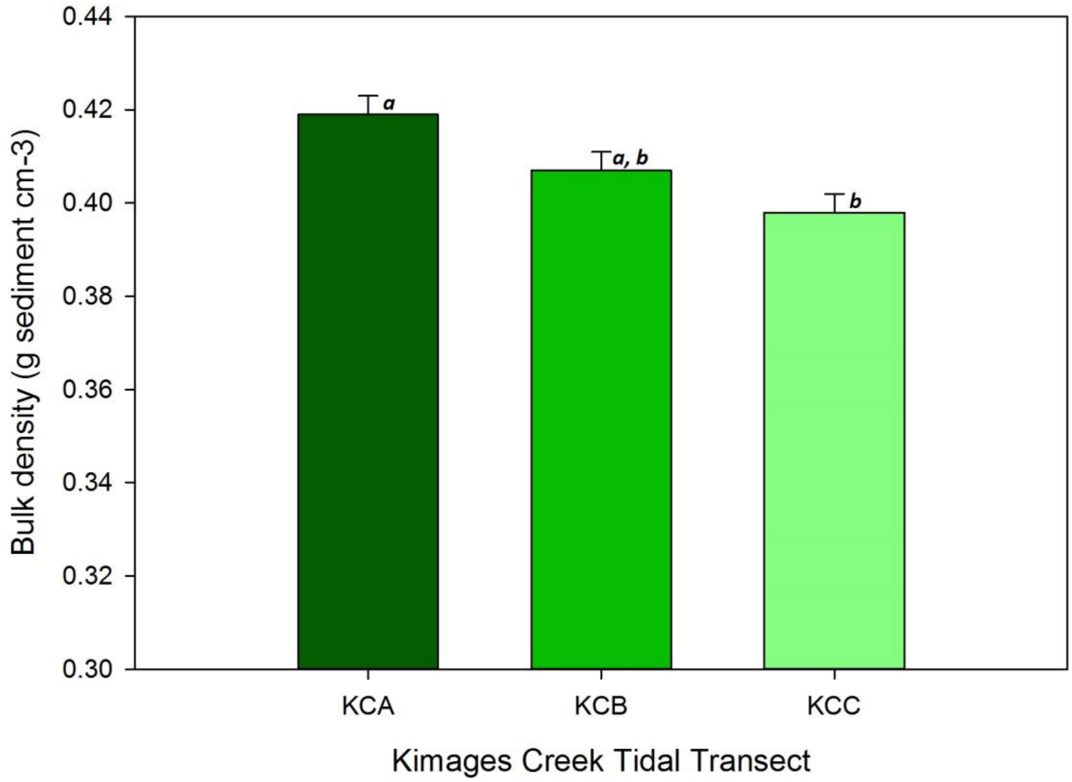

Figure 17. Average bulk density of each tidal transect within Kimages Creek. Data presented are means ± Standard error. Lower case letters indicate significant differences among sites $p<0.05$.

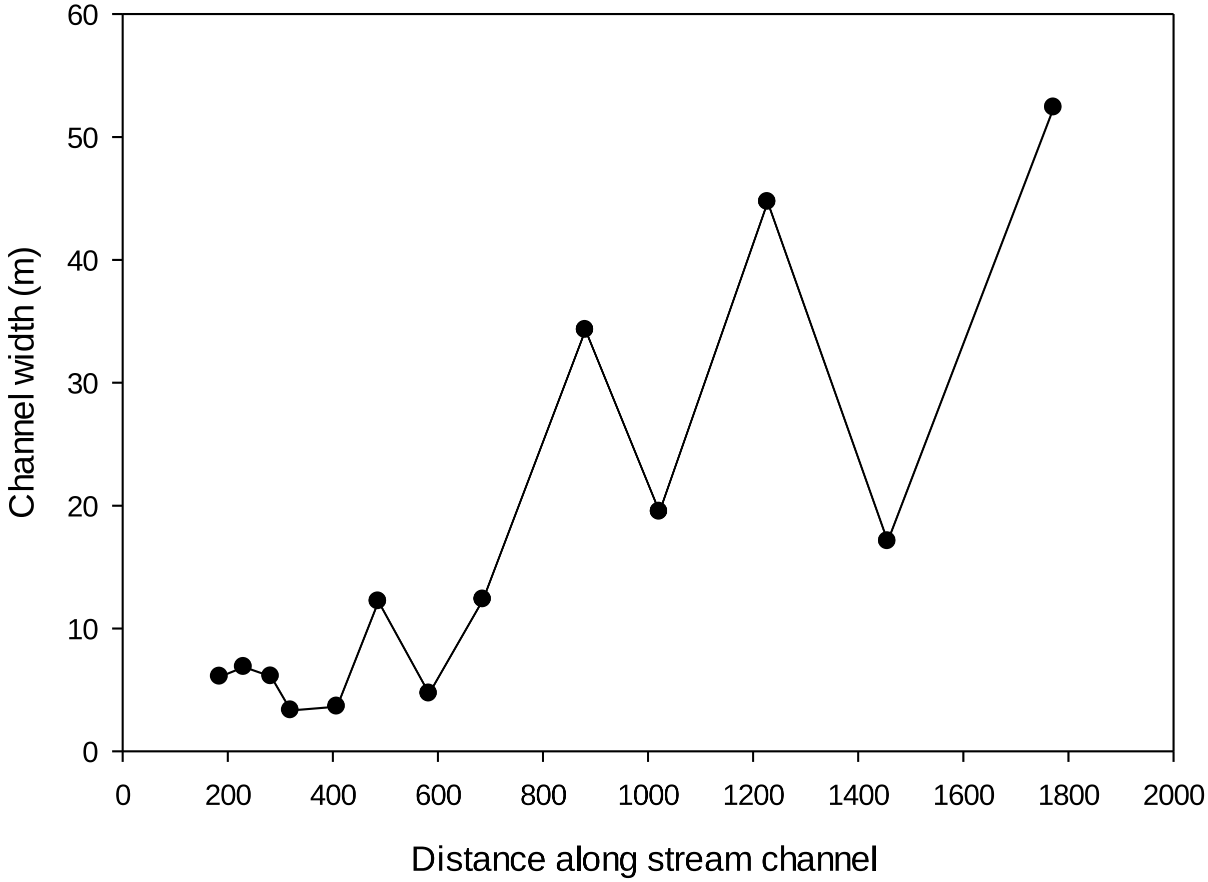

Figure 18: Bank width variation along Kimages Creek (data shown are bank widths at each cross-section).

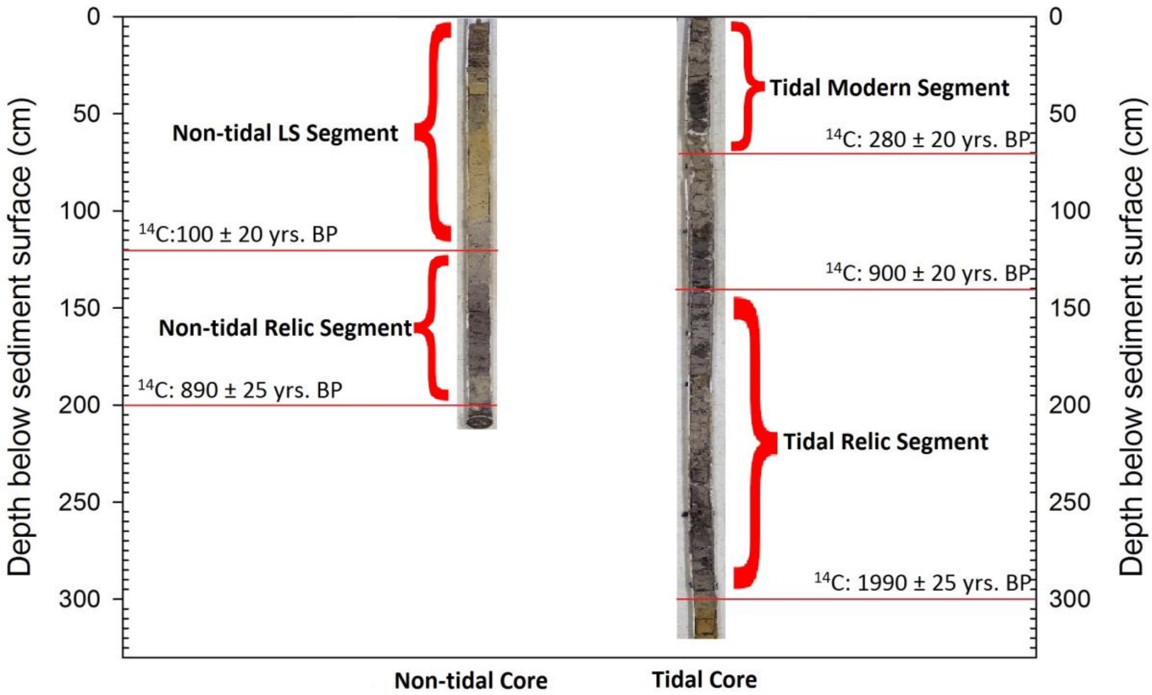

Figure 19. ^{14}C results within Kimages Creek Non-tidal and Tidal sediment cores.

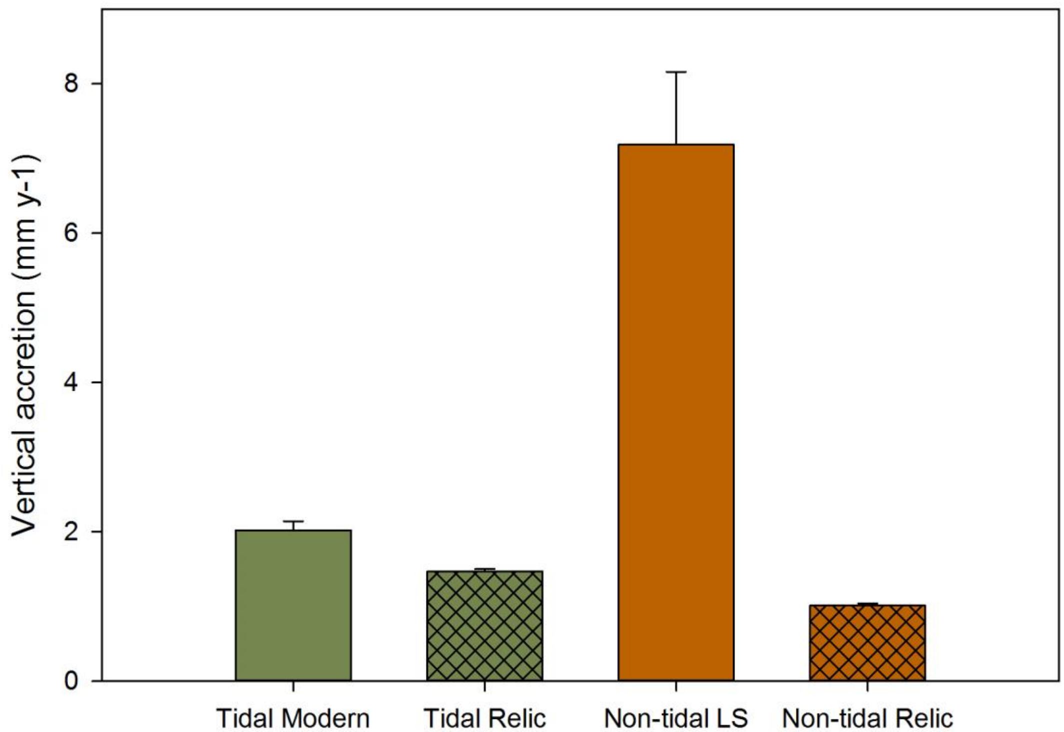

Figure 20. Vertical accretion rates (mm y^{-1}) across tidal and non-tidal sediment cores collected within Kimages Creek. Variations were calculated based on ^{14}C results. Range represents analytical uncertainty associated with radiocarbon dating and conversion to calendar age.

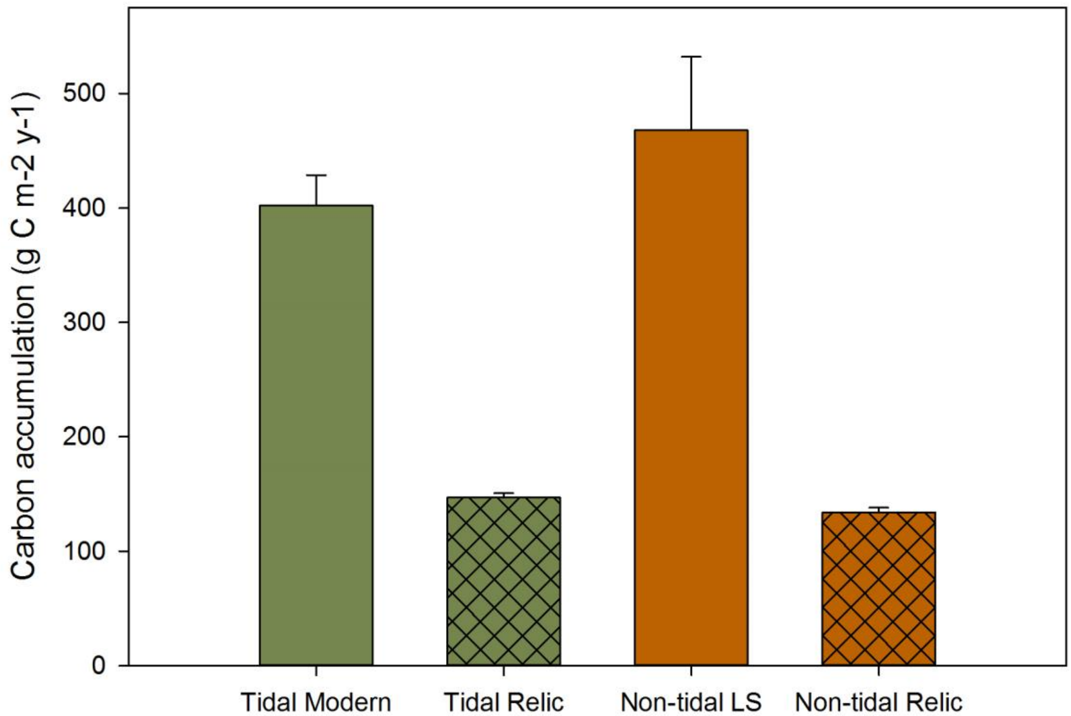

Figure 21. Carbon accumulation rates (g C m^{-2} y^{-1}) across tidal and non-tidal sediment cores within Kimages Creek. Variations were calculated based on ^{14}C results using Equation 2. Range represents analytical uncertainty associated with radiocarbon dating and conversion to calendar age.

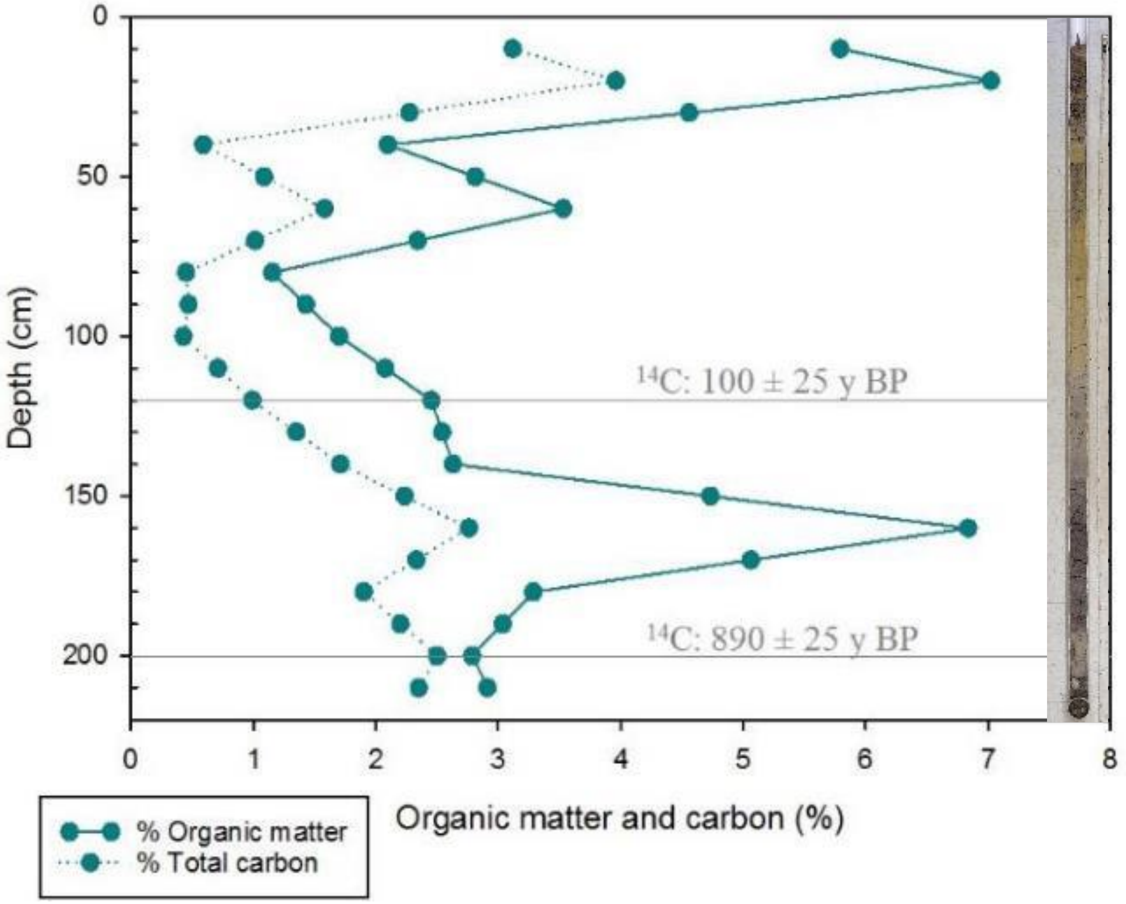

Figure 22. Kimages Creek non-tidal core characterization with sediment organic content, percent carbon, and ^{14}C dates.

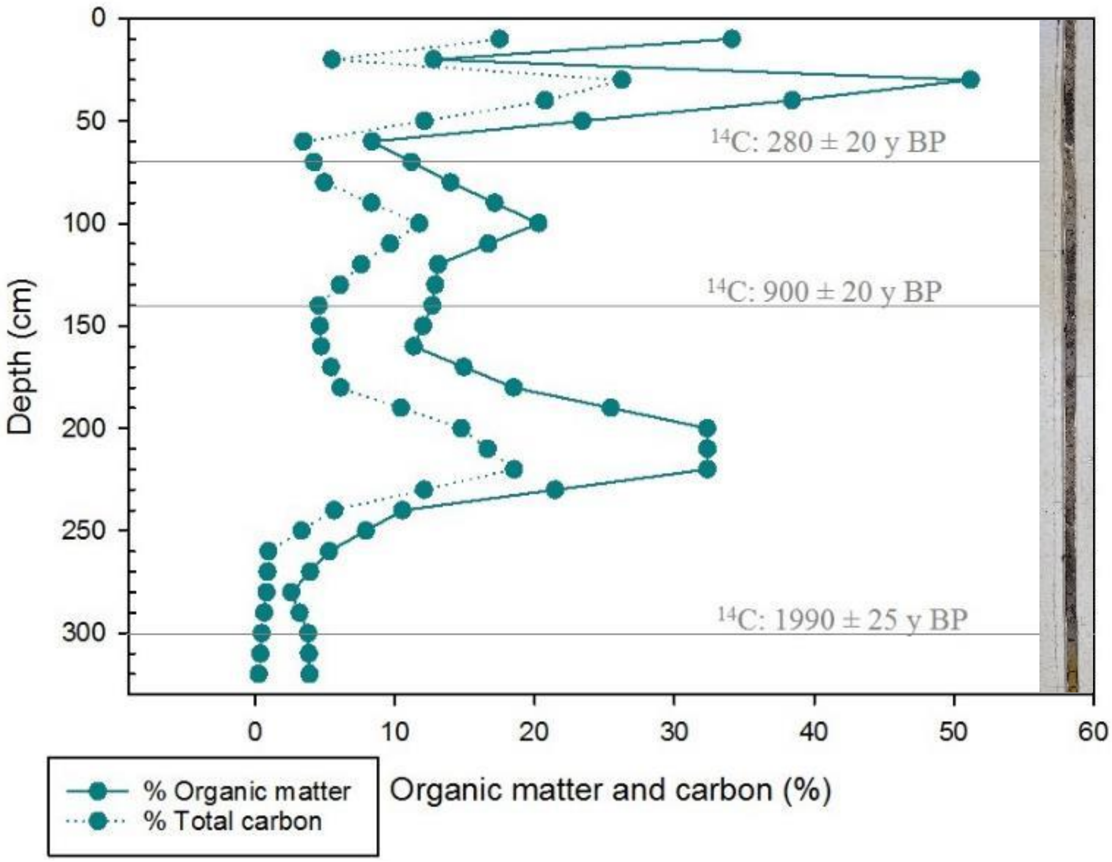

Figure 23. Kimages Creek tidal core characterization with sediment organic content, percent carbon, and ^{14}C dates.

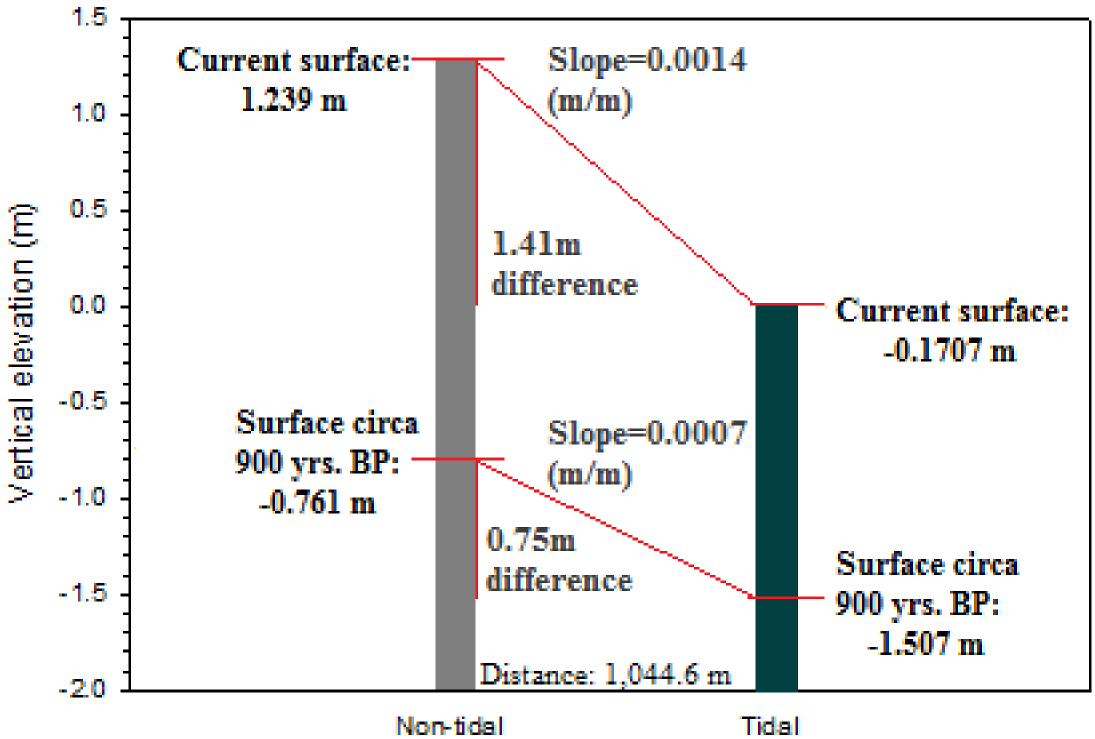

Figure 24: Elevation and slope differences between cores collected within Kimages Creek. Vertical elevation (m) is based on NAVD 88 vertical datum.

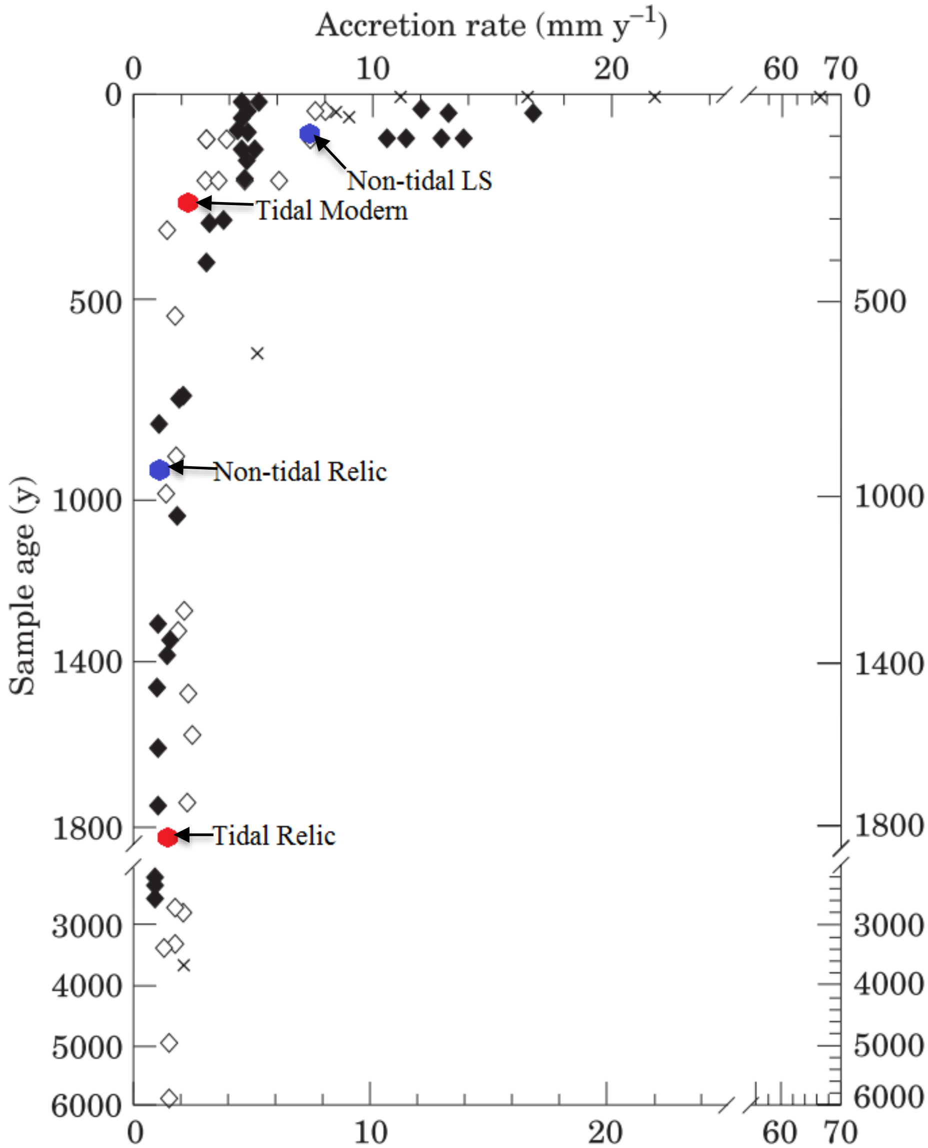

Figure 25. Accretion rate versus sample age for mid-Atlantic tidal marshes (U.S.A.) modified after Nuebauer et al., 2002. Data are presented from studies where accretion rates were measured over a range of time scales. This study (restored tidal and non-tidal freshwater marsh) represented by blue (non-tidal) and red (tidal) hexagons. Other data of tidal freshwater marshes are represented using black diamonds and are from Orson et al. (1990; Delaware River), Khan and Brush (1994; Jug Bay, MD). Tidal freshwater marsh data from Nuebauer et al.,represented using x (2002; Pamunkey River, VA). Salt marsh data points are represented using hallow diamonds and are from Ellison and Nichols (1976; James and Rappahannock Rivers, VA) and Kearney et al. (1994; Monie Bay, MD).

Literature Cited

Baldwin, H., & Mendelssohn, I. (1998). Effects of salinity and water level on coastal marshes: an experimental test of disturbance as a catalyst for vegetational change. *Aquatic Botany*, *61*, 255–268.

Ballantine, K., & Schneider, R. (2009). Fifty-five years of soil development in restored freshwater depressional wetlands. *Ecological Applications*, *19*(6), 1467–1480. https://doi.org/10.1890/07-0588.1

Barendregt, A., & Swarth, C. W. (2013). Tidal Freshwater Wetlands: Variation and Changes. *Estuaries and Coasts*, *36*(3), 445–456. https://doi.org/10.1007/s12237-013-9626-z

Beck, R. W., Inc., (1998). Condit Hydroelectric Project Removal: Summary Report and Engineering Considerations.

Bednarek, A. T. (2001). Undamming rivers: A review of the ecological impacts of dam removal. *Environmental Management*, *27*(6), 803–814. https://doi.org/10.1007/s002670010189

Boon, J. (2005). *Sea Coast and Sea Level Trends*. Retrieved from http://www.vims.edu/research/departments/physical/_docs/sealevel.pdf

Bukaveckas, P. A., and J. Wood. (2014). Nitrogen Retention in a Restored Tidal Stream (Kimages Creek, VA) Assessed by Mass Balance and Tracer Approaches. Journal of Environmental Quality 43:1614.

Butzeck, C., Eschenbach, A., Gröngröft, A., Hansen, K., Nolte, S., & Jensen, K. (2014). Sediment Deposition and Accretion Rates in Tidal Marshes Are Highly Variable Along Estuarine Salinity and Flooding Gradients. *Estuaries and Coasts*, 434–450. https://doi.org/10.1007/s12237-014-9848-8

Christiansen, T., P. L. Wiberg, and T. G. Milligan. (2000). Flow and Sediment Transport on a Tidal Salt Marsh Surface. Estuarine, Coastal and Shelf Science 50:315–331.

Craft, C., Clough, J., Ehman, J., Jove, S., Park, R., Pennings, S., … Machmuller, M. (2009). Forecasting the effects of accelerated sea-level rise on tidal marsh ecosystem services. *Frontiers in Ecology and the Environment*, *7*(2), 73–78. https://doi.org/10.1890/070219

Crawford, E. R., Day, F. P., & Atkinson, R. B. (2007). Influence of environment and substrate quality on root decomposition in naturally regenerating and restored Atlantic white cedar wetlands. *Wetlands*, *27*(1), 1–11. https://doi.org/Doi 10.1672/0277-5212(2007)27[1:Ioeasq]2.0.Co;2

Crawford, E., Day, F., & Atkinson, R. (2005). Decomposition dynamics in an Atlantic White Cider Restoration site, Atlantic White Cider Symposium Proceedings

Crawford, E. (2002). Decomposition dynamics in restored and naturally recovering Atlantic white cedar (*Chamaecyparis thyoides*) wetlands. (Doctoral Dissertation). Retrieved from Old Dominion University These. (ALMA MMS ID 991008280259703186)

Cooper, M., Beever, M., & Oppenheimer, M. (2008). The potential impacts of sea level rise on the coastal region of New Jersey, USA. *Climate Change*, *90*, 475–492. https://doi.org/10.1007/s10584-008-9422-0

D'Alpaos, A., Lanzoni, S., Marani, M., & Rinaldo, A. (2007). Landscape evolution in tidal embayments: Modeling the interplay of erosion, sedimentation, and vegetation dynamics. *Journal of Geophysical Research: Earth Surface*, *112*(1), 1–17. https://doi.org/10.1029/2006JF000537

Deemy, J. B. (2012). *Spatial Patterns of Herbaceous and Woody Recruitment in a Recently Restored Mixed Tidal Regime Freshwater Wetland*. M.S. Thesis, Virginia Commonwealth University.

Donovan, M., Miller, A., Baker, M., & Gellis, A. (2015). Sediment contributions from floodplains and legacy sediments to Piedmont streams of Baltimore County, Maryland. *Geomorphology*, *235*, 88–105. https://doi.org/10.1016/j.geomorph.2015.01.025

Doyle, M., Stanley, E., & Harbor, J. (2002). Geomorphic analogies for assessing probable channel response to dam removal. *Journal of the American Water Resources Association*, *38*(6).

Ensign, S., Siporin, K., Piehler, M., Doyle, M., & Leonard, L. (2013). Hydrologic Versus Biogeochemical Controls of Denitrification in Tidal Freshwater Wetlands. *Estuaries and Coasts*, *36*(3), 519–532. https://doi.org/10.1007/s12237-012-9491-1

Ellison, R. L. & Nichols, M. M. (1976). Modern and Holocene Foraminifera in the Chesapeake Bay Region. First International Symposium on Benthonic Foraminifera of Continental Margins, Halifax, Nova Scotia, Canada. 131–151.

Esselink, P., Dijkema, K. S., Reents, S., & Hageman, G. (1998). Vertical Accretion and Profile Changes in Abandoned Man-Made Tidal Marshes in the Dollard Estuary, the Netherlands. *Journal of Coastal Research*, *14*(2), 570–582. https://doi.org/10.2307/4298810?ref=no-x-route:291008bc12b9f3d703d0d89ecd49352c

Fennessy, M. S., Rokosch, A., & Mack, J. J. (2008). Patterns of plant decomposition and nutrient cycling in natural and created wetlands. *Wetlands*, *28*(2), 300–310. https://doi.org/10.1672/06-97.1

French, J. R. & Spencer, T. (1993). Dynamics of sedimentation in a tide-dominated back barrier salt marsh, Norfolk, UK. *Marine Geology* 110, 315–331.

Gedan, K. B., Kirwan, M. L., Wolanski, E., Barbier, E. B., & Silliman, B. R. (2011). The present and future role of coastal wetland vegetation in protecting shorelines: Answering recent challenges to the paradigm. *Climatic Change*, *106*(1), 7–29. https://doi.org/10.1007/s10584-010-0003-7

Harnois, L., (1988). The CIW index: A new chemical index of weathering: Sedimentary *Geology*, v. 55, p. 319–322. doi:10.1016/0037-0738(88)90137-6

Hedges, J. I. & Keil, R. G. (1995). Sedimentary organic matter preservation: as assessment and speculative synthesis. *Marine Chemistry* 49, 81–115.

Hupp, C. R., Noe, G. B., Schenk, E. R., & Benthem, A. J. (2013). Geomorphology Recent and historic sediment dynamics along Difficult Run, a suburban Virginia Piedmont stream. *Geomorphology*, *180–181*, 156–169. https://doi.org/10.1016/j.geomorph.2012.10.007

Jones, J. (2011). *Putting the environment first*. Retrieved from http://www.vcu.edu/rice/blog/2011/09/putting_the_environment_first.html

Kearney, M. S., Stevenson, J. C., & Ward, L. G. (1994). Spatial and Temporal Changes in Marsh Vertical Accretion Rates at Monie Bay : Implications for Sea-Level Rise *Journal of Coastal Research*, *10*(4), 1010–1020.

Kemp, W. M., W. R. Boynton, J. E. Adolf, D. F. Boesch, W. C. Boicourt, G. Brush, J. C. Cornwell, T. R. Fisher, P. M. Glibert, J. D. Hagy, L. W. Harding, E. D. Houde, D. G. Kimmel, W. D. Miller, R. I. E. Newell, M. R. Roman, E. M. Smith, and J. C. Stevenson. (2005). Eutrophication of Chesapeake Bay: historical trends and ecological interactions. Marine Ecology Progress Series. Marine Ecology Progress Series 303:1–29.

Khan, H., and G.S. Brush. (1994). Nutrient and metal accumulation in a freshwater tidal marsh. *Estuaries* 17: 345–360

Kirwan, M. L., & Megonigal, J. P. (2013). Tidal wetland stability in the face of human impacts and sea-level rise. *Nature*, *504*(7478), 53–60. https://doi.org/10.1038/nature12856

Lyons, N. J., Starek, M. J., Wegmann, K. W., & Mitasova, H. (2015). Bank erosion of legacy sediment at the transition from vertical to lateral stream incision. *Earth Surface Processes and Landforms*, *1778*(June), 1764–1778. https://doi.org/10.1002/esp.3753

Marton, J. M., Fennessy, M. S., & Craft, C. B. (2014). Functional Differences between Natural and Restored Wetlands in the Glaciated Interior Plains. *Journal of Environment Quality*, *43*(1), 409–417. https://doi.org/10.2134/jeq2013.04.0118

McKee, B. A., Nittrouer, C. A. & DeMaster, D. J. (1983). Concepts of sediment deposition and accumulation applied to the continental shelf near the mouth of the Yangtze River. *Geology* 11, 631–633.

Merritts, D., Walter, R., Rahnis, M., Hartranft, J., Cox, S., Gellis, A., … Becker, S. (2011). Anthropocene streams and base-level controls from historic dams in the unglaciated mid-Atlantic region, USA. *Philosophical Transactions of the Royal Society A: Mathematical, Physical and Engineering Sciences*, *369*(1938), 976–1009. https://doi.org/10.1098/rsta.2010.0335

Mitra, S., Wassmann, R., & Vlek, P. L. G. (2005). An appraisal of global wetland area and its organic carbon stock. *Current Science*, *88*(NO. 1), 25–35.

Mitsch, W., and Gosselink, J. (2007). Wetlands. (4th edition). New Jersey: John Wiley & Sons, Inc.

Morris, J. T., Sundareshwar, P. V, Nietch, C. T., Kjerfve, B., & Cahoon, D. R. (2002). Responses of Coastal Wetlands to Rising Sea Level. *Ecology*, *83*(10), 2869–2877.

Morrissey, E. M., Gillespie, J. L., Morina, J. C., & Franklin, R. B. (2014). Salinity affects microbial activity and soil organic matter content in tidal wetlands. *Global Change Biology*, *20*(4), 1351–1362. https://doi.org/10.1111/gcb.12431

Nielsen, N., & Nielsen, J. (2002). Vertical Growth of a Young Back Barrier Salt Marsh , Skallingen, SW Denmark. *Coastal Education & Research Foundation, Inc.*, *1973*(2), 287–299.

Nesbitt, H., & Young, G. (1982). Early Proterozoic climates and plate motions inferred from major element chemistry of lutites. *Nature*, *299*, 715–717.

Neubauer, S. C., Anderson, I. C., Constantine, J. A., & Kuehl, S. a. (2002). Sediment Deposition and Accretion in a Mid-Atlantic (U.S.A.) Tidal Freshwater Marsh. *Estuarine, Coastal, and Shelf Science*, *54*, 713–727. https://doi.org/10.1006/ecss.2001.0854

Neubauer, S. C. (2008). Contributions of mineral and organic components to tidal freshwater marsh accretion. *Estuarine, Coastal and Shelf Science*, *78*(1), 78–88. https://doi.org/10.1016/j.ecss.2007.11.011

Neubauer, S. C., Franklin, R. B., & Berrier, D. J. (2013). Saltwater intrusion into tidal freshwater marshes alters the biogeochemical processing of organic carbon. *Biogeosciences*, *10*(12), 8171–8183. https://doi.org/10.5194/bg-10-8171-2013

Neumeier, U., & Amos, C. L. (2006). The influence of vegetation on turbulence and flow velocities in European salt-marshes. *Sedimentology*, *53*(2), 259–277. https://doi.org/10.1111/j.1365-3091.2006.00772.x

Orson, R. A., Simpson, R. L. & Good, R. E. (1990) Rates of sediment accumulation in a tidal freshwater marsh. *Journal of Sedimentary Petrology* 60, 859–869.

Palinkas, C. M., & Engelhardt, K. A. M. (2016). Spatial and temporal patterns of modern (~100 yr) sedimentation in a tidal freshwater marsh: Implications for future sustainability. *Limnology and Oceanography*, *61*(1), 132–148. https://doi.org/10.1002/lno.10202

Pasternack, G. B., & Brush, G. S. (1998). Sedimentation cycles in a river-mouth tidal freshwater marsh. *Estuaries*, *21*(3), 407–415. https://doi.org/10.2307/1352839

Pasternack, G. B., & Brush, G. S. (2001). Seasonal variations in sedimentation and organic content in five plankt associations on a Chesapeake Bay tidal freshwater delta. *Estuarine Coastal and Shelf Science*, *53*, 93–106. https://doi.org/10.1006

Price, J. R., and M. A. Velbel. (2003). Chemical weathering indices applied to weathering profiles developed on heterogeneous felsic metamorphic parent rocks. Chemical Geology 202:397–416.

Reed, D. J. (2002). Sea-level rise and coastal marsh sustainability: Geological and ecological factors in the Mississippi delta plain. *Geomorphology*, *48*(1–3), 233–243. https://doi.org/10.1016/S0169-555X(02)00183-6

Sallenger, A. H., Doran, K. S., & Howd, P. A. (2012). Hotspot of accelerated sea-level rise on the Atlantic coast of North America. *Nature Climate Change*, *2*(12), 884–888. https://doi.org/10.1038/nclimate1597

Stoker, B. and J.M. Harbor, (1991). Dam removal Methods, Elwha River Wastington. *In:* Hydraulic Engineering, R. M. Shane (Editor). Proceedings of National Conference on Hydraulic Engineering, American Society of Civil Engineers, New York, pp. 668-673.

USACE, National Inventory of Dams. *Washington, DC :US Army Corps of Engineers : Federal Emergency Management Agency. Retrieved January 20, 2017, from http://nid.usace.army.mil/cm_apex/f?p=838:3:0::NO*

US Climate Data, (2017) *Retrieved January 20, 2017, from http://www.usclimatedata.com/climate/hopewell/virginia/united-states/usva0370*

Van Proosdij, D., Ollerhead, J., & Davidson-Arnott, R. G. D. (2006). Seasonal and annual variations in the volumetric sediment balance of a macro-tidal salt marsh. *Marine Geology*, *225*(1–4), 103–127. https://doi.org/10.1016/j.margeo.2005.07.009

Walter, R. C., & Merritts, D. J. (2008). Natural Streams and the Legacy of Water-Powered Mills. *Science*, *319*(5861), 299–304. https://doi.org/10.1126/science.1151716

Weston, N. B. (2014). Declining Sediments and Rising Seas: An Unfortunate Convergence for Tidal Wetlands. *Estuaries and Coasts*, *37*(1), 1–23. https://doi.org/10.1007/s12237-013-9654-z

Weston, N. B., Vile, M. A., Neubauer, S. C., & Velinsky, D. J. (2011). Accelerated microbial organic matter mineralization following salt-water intrusion into tidal freshwater marsh soils. *Biogeochemistry*, *102*(1), 135–151. https://doi.org/10.1007/s10533-010-9427-4

Vita

Melissa Joanne Davis was born on May 12 1991, in Richmond, Virginia, and is an American citizen. She graduated from Hermitage High School, Henrico County, Virginia in 2009. She received her Bachelor of Science in Environmental Studies from Virginia Commonwealth University, Richmond, Virginia in 2013. She worked as a teaching assistant, field technician, and technical analysts of geospatial ecological data throughout her graduate career. She received a Master of Science in Environmental Studies from Virginia Commonwealth University, Richmond, Virginia in 2017.